# 1 Contributions of primary anthropogenic sources and rapid secondary

## 2 transformations to organic aerosol pollution in Nanchang, Central China

- Wei Guo<sup>a, b</sup>, Zicong Li<sup>a, b</sup>, Renguo Zhu<sup>a, b</sup>, Zhongkui Zhou<sup>a</sup>, Hongwei Xiao<sup>c</sup>, Huayun Xiao<sup>c</sup>
- 4 a. School of Water Resources and environmental Engineering, East China University of Technology,
- 5 Nanchang 330013, China
- 6 b. Jiangxi Province Key Laboratory of the Causes and Control of Atmospheric Pollution, East China
- 7 University of Technology, Nanchang 330013, China
- 8 c. School of Agriculture and Biology, Shanghai Jiao Tong University, Shanghai 200240, China
- 9 Correspondence: Huayun Xiao (xiaohuayun@sjtu.edu.cn)

## 10 Abstract

11

12

13

14

15

16

17

18

19

20

21

22

23

24

25

Due to the complex composition of organic aerosols (OAs), identifying their sources and understanding their dynamics remain challenging, particularly in urban environments of China where natural and anthropogenic influences to OAs intersect. This study aimed to clarify the relative contributions of primary emissions and secondary formation to urban OAs and confirm the sources and influencing factors of OA pollution. We analyzed major polar organic compounds in fine particulate matter (PM<sub>2.5</sub>) collected over one year in Nanchang, Central China. Specific biomarkers and diagnostic ratios were applied to characterize OA sources and distribution patterns, while chemical mass balance (CMB) models and tracer-based approaches were used to estimate source contributions. Statistical analyses were conducted to investigate OA characteristics and drivers during winter pollution episodes. Notably, fatty acids, fatty alcohols, and saccharides predominated over lignin, resin products, sterols, glycerol, hydroxy acids, and aromatic acids, with molecular profiles indicating both anthropogenic and biogenic origins. Source apportionment results showed that primary organic carbon (POC) and primary OAs (POAs) contributed 58% of total organic carbon and 23% of PM<sub>2.5</sub> mass, respectively, compared with 8% and 4% from secondary organic carbon (SOC) and secondary OAs (SOAs). Anthropogenic sources dominated, accounting for approximately 90% of POC and POAs as well as 60% of SOC and SOAs. Seasonal patterns revealed stronger biogenic influences in spring—summer, whereas

anthropogenic emissions dominated in autumn—winter. Short-term winter episodes were characterized by rapid secondary formation, facilitated by elevated primary emissions and favorable oxidation conditions, including enhanced light intensity and nitrogen oxides.

29

30

31

32

33

34

35

36

37

38

39

40

41

42

43

44

45

46

47

48

49

50

51

52

26

27

28

#### 1 Introduction

Fine particulate matter (PM), specifically PM with an aerodynamic diameter of <2.5 µm (PM<sub>2.5</sub>), affects the environment and climate, posing severe threats to human health (Huebert et al., 2003; Kanakidou, 2005; Riipinen et al., 2012; Shiraiwa et al., 2017; Yazdani et al., 2021). This is evident in China, which has become a focal point for PM<sub>2.5</sub> pollution, characterized by recurrent haze episodes that have intensified since 2011 (Cao et al., 2012; Zhang et al., 2012; Huang et al., 2014). To tackle this pressing challenge, the Chinese government has implemented various measures, including the Air Pollution Prevention and Control Action Plan in 2013, revisions to the Air Pollution Prevention and Control Law in 2014, and the Three-year Action Plan for Winning the Blue Sky Defense War in 2018. Such initiatives have remarkably reduced PM2.5 levels, with concentrations below 35 µg m<sup>-3</sup> as of 2020 (Figure S1a). However, the challenge persists, particularly during winter, as exemplified by the winter of 2023-2024 when PM<sub>2.5</sub> concentrations in many cities exceeded the national air quality standards (Figures S1b and S1c). This underscores an urgent need for effective air quality management strategies (An et al., 2019; Cao and Cui, 2021; Chen et al., 2021; Wu et al., 2021; Zhang et al., 2024). To address urban  $PM_{2.5}$  pollution, comprehensive investigation of pollutant components, identification of pollution sources, and evaluation of influencing factors are required. Organic components constitute an important part of PM<sub>2.5</sub>, accounting for 30%-50% of its mass, with primary and secondary sources (Huang et al., 2014; Zhang et al., 2016; Haque et al., 2022). Primary organic carbon (POC) or primary organic aerosol (POA) is directly emitted from various sources, including biomass burning, coal combustion, vehicle exhaust, cooking, plant debris, and fungal spores (Guo et al., 2012; Yazdani et al., 2021). Secondary organic carbon (SOC) or secondary organic aerosol (SOA) forms in the atmosphere through the photooxidation of biogenic and anthropogenic volatile organic compounds (BVOCs and AVOCs, respectively) (Lewandowski et al., 2008; Stone et al., 2009). Common biogenic precursors include hemiterpenes, monoterpenes, and sesquiterpenes, whereas typical anthropogenic precursors include toluene

and polycyclic aromatic hydrocarbons (PAHs) (Claeys et al., 2004; Al-Naiema and Stone, 2017; Jaoui et al., 2019). Owing to the complex composition of OAs, their diverse emission sources, and the impact of meteorological conditions and photochemical oxidation processes, OA source identification is complicated (Ding et al., 2013; Zhang et al., 2024). For years, research on the composition and source apportionment of OAs has attracted considerable attention. However, a unified conclusion regarding OA sources, particularly in China's intricate urban environments influenced by natural and anthropogenic factors, remains elusive (Wang et al., 2006; Fu et al., 2008; Guo et al., 2012; Ding et al., 2014; Xu et al., 2022). Various source apportionment methods have been employed. Such methods include the elemental carbon-based and water soluble OC-based methods (EC-based and WSOC-based methods, respectively; Xu et al., 2021), the compound tracer method (tracer-based method; Ding et al., 2014; Ren et al., 2021; Haque et al., 2023), the isotope signature method (Tang et al., 2022; Xu et al., 2022 and 2023; Zhang et al., 2024), and the use of source apportionment models, such as the chemical mass balance (CMB) and positive matrix factorization models (Xu et al., 2021; Zhang et al., 2023). However, these methods yielded different source contributions. The relative significance of primary emissions versus secondary formation in urban OAs continues to be controversial. Further investigation is required to clarify the sources of OA pollution and the influencing factors.

Thus, this research presents a comprehensive assessment of OAs in Nanchang, a city in Central China characterized by moderate PM<sub>2.5</sub> pollution levels that reflect broad urban atmospheric conditions across China (Figure S1). Employing the CMB model and tracer-based method, as well as EC-based method, we quantitatively evaluated the contributions of POC and SOC to OC, as well as the contributions of the corresponding POA and SOA to the mass of PM<sub>2.5</sub>. Results showed that urban OAs were predominantly influenced by anthropogenic sources, with primary contributions exceeding secondary contributions. Based on a continuous year-long observation (November 1, 2020 to October 31, 2021, 365 daily samples), we discovered that the anthropogenic contributions significantly increased in autumn and winter. However, the biogenic contributions increased in spring and summer. Short-term winter pollution episodes were promoted by rapid secondary transformation, primarily due to high primary emissions and favorable oxidation conditions, including increased light intensity and nitrogen oxides (NO<sub>x</sub>). This study integrates multiple source apportionment methods and accounts for the seasonal characteristics of OA pollution, providing a robust

framework for understanding urban air quality dynamics. The findings have implications for governmental strategies for mitigating air pollution and preventing haze episodes in Nanchang and its environs. The insights obtained serve as a future reference for investigating the impacts of organic compounds in  $PM_{2.5}$  on visibility, public health, and climate change.

#### 2 Materials and methods

### 2.1 Sampling sites and sample collection

The study area was Nanchang, Central China, with sampling at the East China University of Technology located in the northwest region of the city (28.72°N, 115.83°E). As detailed in our previous investigations (Guo et al., 2024a and 2024b), the sampling site was in a mixed-use area characterized by educational, commercial, transportation, and residential activities, devoid of significant local pollution sources. The sampler was strategically placed on the rooftop of a six-story building, approximately 20 m in height, ensuring an unobstructed sampling environment.

Sampling was conducted from November 1, 2020, to October 31, 2021, with daily PM<sub>2.5</sub> sample collections. An 8-inch × 10-inch quartz fiber filter (Pall Tissuquartz, USA) was employed in a high-volume air sampler at a flow rate of 1.05 ± 0.03 m<sup>3</sup> min<sup>-1</sup> for sample collection. The meteorological parameters and gaseous pollutant data for the sampling period were obtained from publicly available online monitoring platforms (https://weatherandclimate.info and http://www.aqistudy.cn/). In particular, the meteorological data were retrieved from the ground meteorological observation station at Nanchang Changbei Airport, and gaseous pollutant data were obtained from the air quality monitoring station operated by the Jiangxi Academy of Forestry. These stations are the closest to the sampling site, located approximately 10 km and 2 km away, respectively. Both stations are ground-based, equipped with online monitoring instruments, and situated on open, flat terrain without surrounding buildings or obstructions. A detailed summary of the prevailing meteorological conditions and air quality during the sampling period is provided in Text S1 and Figure S2.

### 2.2 Chemical analyses

The OC and EC concentrations in the PM<sub>2.5</sub> samples were quantified using the Desert Research Institute Model 2001 Carbon Analyzer, following the thermal/optical reflectance protocol established by the Interagency Monitoring of Protected Visual Environments (IMPROVE) (Chow et al., 2007). A 1.0-cm<sup>2</sup> filter sample was

placed in a quartz boat in the analyzer and subjected to incremental heating at predetermined temperatures: 140 °C for OC1, 280 °C for OC2, 480 °C for OC3, and 580 °C for OC4 in a non-oxidizing helium atmosphere; and 580 °C for EC1, 740 °C for EC2, and 840 °C for EC3 in an oxidizing atmosphere containing 2% oxygen in helium. Repeated analyses were performed, demonstrating an analytical uncertainty of ±10%.

We employed methodologies outlined by Wang et al. (2005 and 2006) and Fu et al. (2008 and 2010) for the extraction and derivatization of organic compounds. The involved filter samples underwent three consecutive ultrasonic extractions using a dichloromethane—methanol mixture (2:1 v/v), followed by the concentration and drying of the resulting extracts. Prior to instrumental analyses, N,O-bis-(trimethylsilyl) trifluoroacetamide and pyridine were introduced to derivatize the polar compounds in the extract. The extract species included polar and non-polar organic compounds, and they were simultaneously detected by the involved instrument. We used non-polar C13 n-alkanes as internal standards for quantitative analyses.

The identification and quantification of organic compounds were achieved via gas chromatography—mass spectrometry (GC–MS) using a Thermo Scientific TRACE GC system coupled to a Thermo Scientific ISQ QD single quadrupole mass spectrometer. GC separation was performed using a DB-5MS fused silica capillary column. Text S2 and Table S1 present the parameters for GC–MS analysis, including temperature elevation procedures, qualitative and quantitative methods for the compounds, and quality assurance and control protocols. Polar and nonpolar organic compounds in the extracts were simultaneously analyzed; however, this study focused on the results regarding the polar compounds; the findings related to nonpolar compounds are provided in our earlier publications (Guo et al., 2024a and 2024b).

## 2.3 Source apportionment methods

To quantify the contributions of various primary sources to OC and PM<sub>2.5</sub>, i.e., the POC and POA, we utilized the CMB model (version 8.2), a widely accepted source apportionment method developed by the United States Environmental Protection Agency (Lewandowski et al., 2008; Stone et al., 2009; Guo et al., 2012; Wu et al., 2020; Xu et al., 2021). The model assumes that the chemical composition of pollutants remains unchanged during transport, allowing measured chemical species at the receptor to be expressed as the linear sum of contributions from individual source categories. Accurate CMB results depend critically on the selection of representative emission sources and chemical tracers. These must include all major contributors and feature

chemical markers that are stable during transport and distinct among sources (Stone et al., 2009). To meet these requirements, we first identified four major primary OC sources: biomass burning, coal combustion, vehicular exhaust, and cooking emissions, based on China's atmospheric PM and gaseous pollutant emission inventories (Huang et al., 2015; Li et al., 2019; Tong et al., 2020), We also considered the contributions of plant debris and fungal spores to OC, base on the regional studies on OC sources (Fan et al., 2020; Xu et al., 2020; Wu et al., 2020). Representative source profiles and tracers of these sources were compiled from recent local and regional reports. For example, biomass burning releases substantial amounts of levoglucosan, accounting for ~8.3% of OC in local profiles (Zhang et al., 2007), and was therefore chosen as its marker compound. For coal combustion and vehicular exhaust, both characterized by complex mixtures include nalkanes, polycyclic aromatic hydrocarbons (PAHs), and hopanes (Rogge et al., 1993a; Oros and Simoneit, 2000; Zhang et al., 2008; Cai et al, 2017). Local emission profiles indicated coal combustion tends to emit a higher proportion of 3- to 4-ring PAHs (Zhang et al., 2008), whereas vehicular exhaust is characterized by higher contributions from C20-C22 n-alkanes (Cai et al, 2017). Consequently, we selected 3- to 4-ring PAHs and C20–C22 n-alkanes as the representative organic markers for local coal combustion and vehicle emissions, respectively. Cooking emissions are dominated by fatty acids, particularly saturated palmitic acid (C16:0) and stearic acid (C18:0), as well as unsaturated fatty acids like palmitoleic acid (C16:1) and oleic acid (C18:1). Given the instability of unsaturated fatty acids in ambient air (Kawamura and Gagosian, 1987; Rudich et al., 2007), only the more stable saturated fatty acids—palmitic and stearic acids—were used as characteristic markers for local cooking emissions (He et al., 2004; Zhao et al., 2007 and 2015). For plant debris, emission profiles from Los Angeles area indicate that plants release considerable quantities of long-chain odd-carbon-number n-alkanes (e.g., C25, C27, C29) (Rogge et al., 1993b); however, many local studies indicate that biomass burning, coal combustion, and vehicle exhaust also emit long-chain n-alkanes to some extent (Zhang et al., 2007, 2008; Cai et al., 2017). Overlap among sources diminishes the diagnostic value of long-chain n-alkanes, some investigations have consequently proposed glucose as a more selective tracer for plant debris (Fan et al., 2020; Xu et al., 2021). Puxbaum and Tenze-Kunit (2003) report that glucose comprises approximately 5.2% of plant-derived organic carbon, whereas other sources other than plants rarely emit glucose. On this basis, glucose was adopted here as the plant emission biomarker. Additionally, certain fungal

134

135

136

137

138

139

140

141

142

143

144

145

146

147

148

149

150

151

152

153

154

155

156

157

158

159

160

spores contribute to OC in ambient air; literature reports indicate that particles originating from fungal spores contain abundant mannitol and arabitol, accounting for roughly 13% and 19% of OC, respectively (Bauer et al., 2002, 2008). Accordingly, mannitol and arabitol were chosen as the marker compounds representing fungal spores in this study. Detailed source profile information used in CMB model is provided in Fig. S3 of the supplementary material. It should be noted that the local source profile dataset subdivides major sources—such as coal combustion, vehicle exhaust, and cooking—into multiple categories (for example, industrial versus residential coal burning, gasoline versus diesel exhaust, and regional cooking styles such as Guangdong versus Sichuan). For each major source category, we represented typical source characteristics by using either the mean profile of its subcategories or the average profile derived from multiple observational studies. Similarly, using the proportions of characteristic species in PM<sub>2.5</sub> from these emission source profiles, the CMB model subsequently estimated each source's contribution to PM<sub>2.5</sub>. In the primary emission profiles applied here, the PM-to-OC ratio ranged from 1.42 to 2.15.

To assess the contributions of various secondary sources to OC and  $PM_{2.5}$ , i.e., SOC and SOA concentrations, we employed tracer-based method, a well-established method for SOC and SOA source apportionment. The tracer-based method operates on principles analogous to those involved in the CMB model, relying on the mass fractions of characteristic tracers in SOC ( $f_{SOC}$ ) and SOAs ( $f_{SOA}$ ) from emission sources to ascertain the contributions of different sources. The SOC and SOA tracer-based method was first proposed and utilized by Kleindienst et al. (2007 and 2012). Its specific calculation procedure is as follows:

$$[SOC] = \frac{\sum_{i} [tr_{i}]}{f_{SOC}}, \tag{1}$$

$$[SOA] = \frac{\sum_{i} [tr_i]}{f_{SOA}}, \tag{2}$$

where  $\Sigma$ i[tri] is the total concentration of the selected tracers in the sample, denoting representative compounds from specific emission categories;  $f_{SOC}$  and  $f_{SOA}$  are the mass fractions of the tracers in OC and PM<sub>2.5</sub> from secondary emissions, respectively. The values of  $f_{SOC}$  and  $f_{SOA}$  are determined according to the chamber experiments conducted, in which gaseous precursors are transformed into SOC and SOAs under oxidative and illuminative conditions. Herein, we employed six compounds associated with hemiterpenes, four compounds related to monoterpenes, as well as  $\beta$ -caryophyllinic acid, 2,3-dihydroxy-4-oxopentanoic acid, and

phthalic acid as marker compounds to indicate the contributions of different biogenic (hemiterpenes, monoterpenes, and sesquiterpenes) and anthropogenic (toluene and naphthalene) sources to SOC and SOA. We adopted the  $f_{SOC}$  and  $f_{SOA}$  values used by Kleindienst et al. (2007 and 2012). to calculate the SOC and SOA concentrations originating from various sources. All marker selections, f-values, and the conversion coefficients between  $f_{SOA}$  and  $f_{SOC}$  derived from chamber studies are listed in Table S2, and the calculations assume that the chamber-derived SOC and SOA relationships are representative of the relevant atmospheric oxidation regimes, acknowledging associated uncertainties.

Furthermore, we employed the EC-based method to estimate the total POC and SOC concentrations, enabling a comparison with the POC and SOC concentrations obtained using the tracer-based method. This method uses EC as a tracer for POC and approximates the observed minimum ratio of OC to EC (OC/EC)<sub>min</sub> as an equivalent to the primary emission OC/EC value (OC/EC)<sub>pri</sub> (Turpin and Huntzicker, 1995; Castro et al., 1999). The equation used for estimating SOC is

$$SOC_{EC-based} = OC - EC \times (OC/EC)_{min}, \tag{3}$$

- where the minimum OC/EC values observed in spring, summer, autumn, and winter were 2.01, 2.20, 2.15, and
- 201 2.31, respectively.

202 3 Results and discussion

## 3.1 Carbonaceous components

The OC and EC concentrations were in ranges of 1.01–13.66 (mean:  $5.88 \pm 2.57 \,\mu g \, m^{-3}$ ) and 0.27–4.55  $\mu g \, m^{-3}$  (mean:  $1.75 \pm 0.88 \,\mu g \, m^{-3}$ ), respectively. Seasonal variations in the OC and EC concentrations closely mirrored those observed for PM<sub>2.5</sub>, with elevated levels in autumn and winter and diminished levels in spring and summer (Figure 1a). Owing to its stability and resistance to chemical transformations in the atmosphere, EC is frequently employed as a tracer for primary emissions. The OC/EC ratio is a useful tool for assessing the relative contributions of primary and secondary sources (Castro et al., 1999; Turpin and Huntzicker, 1995). Generally, an OC/EC value above 2 indicates a predominant contribution of secondary sources to OC, whereas values below 2 suggest greater contributions from primary sources (Kunwar and Kawamura, 2014). Here, the majority of the OC/EC values exceeded 2 (Figure 1b), implying that the OC may have been significantly influenced by secondary sources. The OC/EC values were relatively high in summer (4.33  $\pm$  2.07) and winter

 $(4.18 \pm 2.57)$  compared with those observed in spring  $(3.36 \pm 1.98)$  and autumn  $(3.59 \pm 1.22)$ . This indicates an increased contribution to OC from secondary sources during the summer and winter.

## 3.2 Major polar components

#### 3.2.1 Fatty acids

214

215

216

217

218

219

220

221

222

223

224

225

226

227

228

229

230

231

232

233

234

235

236

237

238

239

240

A range of homologous straight-chain C10:0-C32:0 fatty acids (FAs) and unsaturated C16:1 and C18:1 FAs were detected in the PM<sub>2.5</sub> samples (Figures 1c and 2a). Their distribution exhibited a strong even-carbonnumber predominance, as indicated by a carbon preference index (CPI) of  $7.59 \pm 7.42$  (Figure S4a), with peaks at C16:0 and C18:0. The total FA concentration was in a range of 3-658 ng m<sup>-3</sup>, with an average concentration of 197± 111 ng m<sup>-3</sup>. Similar molecular distribution patterns and concentrations have been documented in urban aerosol studies across China (59-2,090 ng m<sup>-3</sup>; He et al., 2004 and 2006; Wang et al., 2006; Haque et al., 2019; Fan et al., 2020). In these Chinese cities, FAs are primarily influenced by biogenic sources, including plant releases and biomass burning, as well as fossil fuel combustion and residential cooking. This average concentration generally exceeds those observed for coastal and marine aerosol samples (0.1–160 ng m<sup>-3</sup>; Kawamura et al., 2003; Wang et al., 2007; Fu et al., 2011), which are primarily influenced by marine biological activities and long-range transport of continental sources. High-molecular-weight FAs (HFAs,  $\geq$  C20:0) are typically derived from the waxes of terrestrial higher plants or biomass burning, whereas low-molecularweight FAs (LFAs, < C20:0) originate from more diverse sources, including vascular plants, microorganisms, marine phytoplankton, and kitchen emissions (Fu et al., 2008 and 2010). Consequently, the ratio of LFAs to HFAs (LFA/HFA ratio) is an indicator of the relative contributions from various sources. Here, the LFA/HFA range was 0.34-10.67, with an average of  $2.45 \pm 1.53$  (Figure S4b), suggesting that the FAs may have originated from a mixture of natural and anthropogenic sources. The specific FAs C16:0 and C18:0 are associated with different sources. C16:0 is primarily derived from biomass burning or plant emissions, whereas C18:0 predominantly originates from vehicle exhaust, cooking emissions, or road dust (Wang et al., 2007; Fu et al., 2010). Thus, the ratio of C18:0 to C16:0 (C18:0/C16:0) is frequently employed to assess the FA source. A C18:0/C16:0 ratio below 0.25 suggests a primary contribution from biomass burning or plant emissions, whereas ratios between 0.25 and 0.5 indicate a predominant influence from vehicle exhaust. C18:0/C16:0 ratios within a range of 0.5-1 suggest a significant contribution from cooking emissions or road dust (Rogge et al., 2006). Here, the C18:0/C16:0 ratio varied from 0.05 to 9.53, with an average value of 0.59  $\pm$  0.88 (Figure S3c), indicating that the FAs in Nanchang originated from a mixture of sources.

The average concentrations of unsaturated FAs, specifically C16:1 and C18:1, were  $7 \pm 4$  and  $4 \pm 3$  ng m<sup>-3</sup>, respectively. Such unsaturated FAs are primarily derived from biomass burning, plant leaf emissions, cooking activities, and release from marine organisms (Kawamura and Gagosian, 1987; Rogge et al., 1993b; Nolte et al., 1999). Upon emission into the atmosphere, unsaturated FAs undergo rapid oxidation by ozone (O<sub>3</sub>), hydrogen peroxide (H<sub>2</sub>O<sub>2</sub>), or hydroxyl (OH) radicals. Consequently, the ratio of unsaturated FAs to saturated FAs, represented as (C16:1 + C18:1)/(C16:0 + C18:0), is an indicator of the reactivity and degree of aging of unsaturated FAs (Rudich et al., 2007; Kawamura and Gagosian, 1987). Here, this ratio was  $0.12 \pm 0.06$  (Figure S3d), indicating that the unsaturated FAs underwent significant photochemical degradation and that secondary organic compounds may be common in PM<sub>2.5</sub>.

The average concentrations of most FAs were significantly (p < 0.05) higher in autumn and winter than in spring and summer (Figure 2a), indicating a substantial increase in fatty acid emissions during autumn and winter. The LFA/HFA and C18:0/C16:0 ratios were lower in autumn and winter than in summer (Figures S4b and S4c). This indicated that in autumn and winter, FAs were significantly influenced by terrestrial plant or biomass burning, whereas in summer, they were more influenced by vehicular emissions, marine phytoplankton, and cooking emissions. Conversely, the (C16:1 + C18:1)/(C16:0 + C18:0) values were higher in winter than in summer (Figure S4d). This suggested that unsaturated FAs experienced a greater degree of photochemical degradation during the warm seasons. Unsaturated FAs can be rapidly oxidized by ozone or OH radicals. The higher temperatures, relatively stronger solar radiation, and higher concentrations of  $O_3$  and OH radicals in the summer season will facilitate the oxidative decomposition of unsaturated FAs (Wang et al., 2006; Fan et al., 2020).

#### 3.2.2 Fatty alcohols

Several straight-chain n-alkanols (C14–C32) were detected (Figures 1c and 2b), exhibiting a predominance of even carbon numbers, as indicated by a CPI of  $10.28 \pm 17.05$  (Figure S4e). Low-molecular-weight alcohols (LMW<sub>alc</sub>,  $\leq$  C20) exhibited peaks at C16 and C18, and high-MW alcohols (HMW<sub>alc</sub>, > C20) exhibited peaks at C26, C28, and C30 (Figure 2b). The total concentration of n-alkanols was in a range of 6–572 ng m<sup>-3</sup> (average

= 114  $\pm$  93 ng m<sup>-3</sup>). This concentration fell within the range of reported n-alkanol concentrations in urban aerosols in China (3–1,301 ng m<sup>-3</sup>; Wang et al., 2006; Haque et al., 2019; Fan et al., 2020) and generally exceeded that of coastal and marine aerosol samples (0.1–19.7 ng m<sup>-3</sup>; Kawamura et al., 2003; Fu et al., 2011). In urban aerosols of China, fatty alcohols are primarily derived from vegetation releases, biomass burning, and resuspension of soil particles. The fatty alcohols in coastal and marine aerosols are primarily attributed to the long-range transport of terrestrial soil and biomass burning as well as marine biogenic sources. HMW<sub>alc</sub> primarily originates from higher plant leaf waxes, loess deposits, or biomass burning, and LMW<sub>alc</sub> primarily originates from soil and marine microorganisms (Simoneit, 2002; Kawamura et al., 2003). Here, the LMW<sub>alc</sub> concentration (75  $\pm$  61 ng m<sup>-3</sup>) exceeded that of HMW<sub>alc</sub> (39  $\pm$  34 ng m<sup>-3</sup>), yielding an average LMW/HMW ratio of 2.50  $\pm$  1.73 (Figure S4f), indicating a mixture of n-alkanols from soil, marine organisms, and biomass burning.

The average concentrations of most fatty alcohols were significantly (p < 0.05) higher in autumn and winter than in summer (Figure 2b), indicating a substantial increase in fatty alcohols emissions during autumn and winter. The LMW/HMW values were relatively low in autumn and winter and higher in spring and summer (Figure S4f). This suggests an increased contribution of soil and marine organisms to n-alkanols in spring and summer. Contributions from plant or biomass burning increased in autumn and winter. In Chinese cities, rising temperatures in spring increase soil microbial activity, with marine air masses exerting a stronger influence during summer, potentially increasing emissions from soil and marine organisms in these seasons. In contrast, autumn and winter coincide with the crop harvest and increased winter heating, leading to likely increases in biomass burning emissions during these periods (Wang et al., 2006; Haque et al., 2019; Fan et al., 2020).

## 3.2.3 Saccharides

We investigated three saccharide classes: anhydrosugars, primary sugars, and sugar alcohols. Among the anhydrosugars, levoglucosan had the highest concentration ( $102 \pm 79 \text{ ng m}^{-3}$ ). We observed markedly lower concentrations of mannosan ( $4 \pm 4 \text{ ng m}^{-3}$ ) and galactosan ( $2 \pm 3 \text{ ng m}^{-3}$ ) (Figure 2c). Levoglucosan—a prominent biomarker for biomass burning—has been extensively investigated in urban aerosol samples, with concentrations in a range of 22–2,706 ng m<sup>-3</sup> (Wang and Kawamura, 2005; Wang et al., 2006; Fu et al., 2010; Haque et al., 2019; Fan et al., 2020), indicating the significant influence of biomass burning on the urban

atmosphere. The widespread detection of levoglucosan in various environments—including suburban (10–482 ng m<sup>-3</sup>; Yttri et al., 2007; Fu et al., 2008), marine (0.2–30 ng m<sup>-3</sup>; Simoneit et al., 2004a; Fu et al., 2011), and polar regions (0–3 ng m<sup>-3</sup>; Stohl et al., 2007; Fu et al., 2009)—indicates its potential for long-range atmospheric transport. Compared to those of the major polar organic compounds found in marine environments, such as FAs, fatty alcohols, and saccharides, the concentrations of these substances in urban PM<sub>2.5</sub> are substantially higher. This is primarily attributed to the substantial impact of anthropogenic activities in urban environments—such as vehicle emissions, industrial processes, and residential heating and cooking—all of which can release these major polar components (Wang et al., 2006; Fu et al., 2008; Haque et al., 2019; Fan et al., 2020). In contrast, the organic matter in marine PM<sub>2.5</sub> originates from relatively simpler sources with lower emissions, mainly influenced by natural processes, including marine biological activity and the long-range transport of continental pollutants (Kawamura et al., 2003; Simoneit et al., 2004a; Wang et al., 2007; Fu et al., 2011).

Seasonal variations of anhydrosugars exhibited consistent patterns, with elevated concentrations in autumn

Seasonal variations of anhydrosugars exhibited consistent patterns, with elevated concentrations in autumn and winter and reduced levels in spring and summer (Figure 2c). This indicated increased biomass burning during the cold months. The sources were characterized using levoglucosan-to-mannosan (L/M) and mannosan-to-galactosan (M/G) ratios. Research suggests distinct L/M ranges for different biomass burning sources: softwood (3–10), hardwood (13–35), and agricultural crop burning (40–56) (Oros and Simoneit, 2001; Sheesley et al., 2003; Engling et al., 2014). Coal combustion can produce significant amounts of levoglucosan (Sheesley et al., 2003; Fabbri et al., 2009), typically with higher L/M values (12–189) because of the lower cellulose content compared with that of plant materials (Rybicki et al., 2020a and 2020b). Conversely, M/G values are generally higher for softwood and hardwood combustion at 3.6–7.0 and 1.2–2.0, respectively. However, M/G values are relatively low for agricultural crop burning (0.3–0.6) (Oros and Simoneit, 2001; Sheesley et al., 2003). Here, most samples exhibited relatively high L/M ratios (4.63–466.61, average = 40.22 ± 49.82) and relatively low M/G ratios (0.30–9.41, average = 2.34 ± 1.36). The L/M and M/G ratios were similar to those of previous observations in the urban area of Nanchang (L/M = 7.9–359.1; average = 59.9; Zhu et al., 2022) and fell within the ranges for crop residue burning and coal combustion. This suggests that the dehydrosugars in the PM<sub>2.5</sub> of Nanchang were likely primarily derived from crop residue burning and coal

combustion. In autumn and winter, the contributions of crop residue burning and coal combustion were more prominent, as evidenced by the higher L/M ratios and lower M/G ratios observed compared with those in spring and summer (Figures S4g and S4h).

Primary sugars and sugar alcohols serve as tracers for primary biological aerosol particles, originating from biogenic emissions, including the release of microorganisms, plants, and flowers, as well as the resuspension of surface soils and unpaved road dust containing biological materials (Graham et al., 2003; Simoneit et al., 2004b; Yttri et al., 2007). Furthermore, biomass burning is a notable source of primary sugars and sugar alcohols (Fu et al., 2012). We identified nine primary sugars (ribose, fructose, galactose, glucose, sucrose, lactulose, maltose, turanose, and trehalose; Figure 2c). Glucose ( $15 \pm 7 \text{ ng m}^{-3}$ ) and sucrose ( $15 \pm 6 \text{ ng m}^{-3}$ ) exhibited the highest concentrations, followed by fructose ( $11 \pm 5 \text{ ng m}^{-3}$ ), trehalose ( $11 \pm 1 \text{ ng m}^{-3}$ ), and maltose ( $11 \pm 1 \text{ ng m}^{-3}$ ). The concentrations of galactose ( $11 \pm 1 \text{ ng m}^{-3}$ ), ribose ( $11 \pm 1 \text{ ng m}^{-3}$ ), and lactulose ( $11 \pm 1 \text{ ng m}^{-3}$ ) were comparatively low. We detected four sugar alcohols (mannitol, arabitol, pinitol, and inositol). Mannitol ( $11 \pm 1 \text{ ng m}^{-3}$ ) exhibited the highest concentration, followed by pinitol ( $11 \pm 1 \text{ ng m}^{-3}$ ) and arabitol ( $11 \pm 1 \text{ ng m}^{-3}$ ). The concentration of inositol ( $11 \pm 1 \text{ ng m}^{-3}$ ) was low.

Levoglucosan serves as a specific biomarker for biomass burning, enabling the assessment of biomass burning contributions to sugar compounds through the ratio of levoglucosan to OC (Lev/OC) and the proportion of levoglucosan in the total sugar compounds (Lev%). Typically, a Lev/OC ratio of >0.048 and a Lev% of >68% indicate a dominance of biomass burning. Conversely, values below these thresholds suggest that in addition to biomass burning, other sources, such as biogenic emissions, significantly contribute to the presence of sugar compounds (Yan et al., 2019 and references therein). Here, the Lev% and Lev/OC values were 53.57% ± 17.93% and 0.016 ± 0.009 (Figures S4i and S4j), respectively, indicating that the sugar compounds were influenced by biomass burning and biogenic emissions, particularly the primary sugars and sugar alcohols. Primary sugars, such as glucose and trehalose, as well as the mannitol in sugar alcohol, positively correlated with levoglucosan (Figure S5a). This confirmed that biomass burning may be a potential source of primary sugars and sugar alcohols. However, the correlation was not statistically significant, suggesting that biological sources remain an important contributor to these compounds in Nanchang. The Lev/OC and Lev% values were higher in autumn and winter than in spring and summer (Figures S4i and S4i).

further indicating that biomass burning contributions increased during the cold months. As previously noted, the primary reason for increased biomass burning emissions during the cold season is that autumn marks the crop harvest in China, leading to more straw burning. Furthermore, the temperature decrease in winter results in additional biomass burning for heating purposes.

## 3.3 Minor polar components

## 3.3.1 Lignin, resin products, and sterols

Here, we detected four types of lignin and resin-derived compounds: 4-hydroxybenzoic acid, dehydroabietic acid, vanillic acid, and syringic acid (Figures 1c and 3a). These are generally considered to originate from natural plant release and burning. The burning of coniferous trees, such as pine, releases higher concentrations of dehydroabietic acid than other lignin and resin-derived compounds (Simoneit, 2002). Here, the concentrations of 4-hydroxybenzoic acid ( $5 \pm 4$  ng m<sup>-3</sup>) and dehydroabietic acid ( $3 \pm 2$  ng m<sup>-3</sup>) were high, whereas those of vanillic acid ( $2 \pm 1$  ng m<sup>-3</sup>) and syringic acid ( $2 \pm 1$  ng m<sup>-3</sup>) were relatively low. A significant positive correlation was observed between the total concentration of lignin and resin-derived compounds and levoglucosan (r = 0.80, p < 0.01, Figure S5a), suggesting that biomass burning was a potential source of lignin and resin-derived compounds. The concentration of dehydroabietic acid was significantly lower than that of 4-hydroxybenzoic acid, similar to the pattern observed for Nanjing aerosols (Haque et al., 2019). This implies that coniferous tree combustion may not be the primary source of lignin and resin acids in this region.

We identified several sterols (cholesterol, stigmasterol, and  $\beta$ -sitosterol; average concentrations =  $5 \pm 3$ ,  $5 \pm 4$ , and  $10 \pm 8$  ng m<sup>-3</sup>, respectively; Figure 3a). These sterols originate from distinct sources. Cholesterol, an animal-derived sterol, is primarily associated with meat cooking in the atmosphere (Rogge et al., 1991; Nolte et al., 1999; He et al., 2004). Contrarily, stigmasterol and  $\beta$ -sitosterol are plant-derived sterols, typically originating from plant leaves, cooking, or biomass burning (Nolte et al., 2001; He et al., 2004; Zhao et al., 2007). Here, stigmasterol and  $\beta$ -sitosterol exhibited a significant positive correlation with levoglucosan (Figure S5a). This suggests that biomass burning may be a potential source of plant-derived sterols. The concentrations of stigmasterol and  $\beta$ -sitosterol were higher in autumn and winter than in spring and summer, indicating an increased contribution of biomass burning to sterols in autumn and winter.

#### 3.3.2 Glycerol, hydroxy acids, and aromatic acids

Glycerol and three hydroxy acids, glycolic acid, malic acid, and citric acid, were detected in the PM<sub>2.5</sub> samples (Figures 1c and 3b). The concentration of glycerol was relatively high ( $10 \pm 4 \text{ ng m}^{-3}$ ), whereas the three hydroxy acids exhibited comparable and relatively low concentrations: glycolic acid (7 ± 2 ng m<sup>-3</sup>), malic acid  $(7 \pm 2 \text{ ng m}^{-3})$ , and citric acid  $(6 \pm 2 \text{ ng m}^{-3})$ . These concentrations aligned with reported ranges for urban aerosols (2-146 and 1-180 ng m<sup>-3</sup> for glycerol and hydroxy acids, respectively; Wang et al., 2006; Fu et al., 2010; Haque et al., 2019; Fan et al., 2020). The source of glycerol in urban aerosols is similar to that of sugar alcohols, primarily originating from the emission from plants, the resuspension of surface soils and unpaved road dust containing biological materials, and biomass burning (Simoneit et al., 2004a and 2004b; Fu et al., 2008), whereas glycolic, malic, and citric acids mainly originate from the secondary photooxidation of organic compounds in the atmosphere, such as biogenic unsaturated FAs, cyclic olefins, and isoprene (Kawamura and Ikushima, 1993; Kawamura and Sakaguchi, 1999; Claeys et al., 2004, Haque et al., 2019). No significant correlation was observed between glycerol and the hydroxy acids; however, a notable correlation was observed among the hydroxy acids (r = 0.49-0.66, p < 0.01, Figure S5b). This confirmed the divergent sources of glycerol and hydroxy acids and similar origins for the hydroxy acids. In summer, the concentrations of the hydroxy acids exceeded those in other seasons (Figure 3b). A positive correlation was observed between the polyacids and temperature (r = 0.35–0.51, p < 0.01), suggesting enhanced secondary photochemical oxidation in the warm months. The secondary formation of hydroxy acids in the atmosphere is suggested to be related to the ozone-driven oxidation of organic compounds. Elevated ozone levels and stronger solar radiation during the summer season create more favorable conditions for the secondary production of hydroxy acids (Kawamura and Ikushima, 1993; Kawamura and Sakaguchi, 1999; Claeys et al., 2004). We detected four aromatic acids in the PM<sub>2.5</sub> samples: benzoic acid, phthalic acid, isophthalic acid, and

376

377

378

379

380

381

382

383

384

385

386

387

388

389

390

391

392

393

394

395

396

397

398

399

400

401

402

We detected four aromatic acids in the PM<sub>2.5</sub> samples: benzoic acid, phthalic acid, isophthalic acid, and terephthalic acid at concentrations of  $0.8 \pm 0.3$ ,  $6.4 \pm 4.1$ ,  $1.1 \pm 0.7$ , and  $10.1 \pm 3.1$  ng m<sup>-3</sup>, respectively (Figure 3b). Aromatic acids significantly contribute to the formation of atmospheric particles. Benzoic acid is recognized as a major pollutant in vehicle exhaust and the secondary photochemical oxidation product of aromatic hydrocarbons from vehicle emissions (Kawamura and Kaplan, 1987; Rogge et al., 1993a; Kawamura et al., 2000). Phthalic acid typically originates from the secondary transformation of PAHs, including naphthalene and other PAHs. Terephthalic acid is primarily produced through terephthalate hydrolysis during

the combustion of urban plastics (Fu et al., 2010; Haque et al., 2019). Here, phthalic and terephthalic acids jointly accounted for approximately 90% of the total detected aromatic acids. A significant positive correlation was observed between phthalic acid and PAHs (r = 83, p < 0.01), as well as between terephthalic acid and the total phthalates (r = 0.72, p < 0.01). The PAH and phthalate data have been published by Guo et al. (2024a and 2004b). This suggests that the secondary conversion of PAHs and the hydrolysis of phthalates (specifically terephthalate) during plastic burning significantly contribute to aromatic acid levels. The phthalic acid concentrations were higher in autumn and winter, whereas terephthalic acid levels peaked in spring and summer (Figure 3b). This indicates that the secondary transformation of PAHs was more pronounced during the cold months, whereas high temperatures in spring and summer promoted the volatilization and transformation of phthalates from plastic sources. Phthalates are employed as plasticizers in resins and polymers. Because they are not chemically bound to the polymer matrix, they can be easily released into the air through evaporation. Higher ambient temperatures in spring and summer favor phthalate release from the matrix (Wang et al., 2006; Fu et al., 2010).

## 3.4 SOA tracers in PM<sub>2.5</sub>

## 3.4.1 Biogenic SOA tracers

Biogenic and anthropogenic SOAs are critical in influencing the atmospheric radiation balance and regional air quality (Ding et al., 2014). Biogenic SOA tracers include oxidation products from isoprene, monoterpenes, sesquiterpenes, and other oxygenated hydrocarbons. Isoprene is the dominant component of BVOC emissions, accounting for ~45% of the total emissions (annual release estimated at 600 Tg C) (Piccot et al., 1992; Guenther et al., 1995; Sharkey et al., 2008). Here, we detected six isoprene oxidation products (2-methylglyceric acid (2-MGA), three C5-alkene triols, and two 2-methyltetrols (MTLs) at concentrations of 1.8  $\pm$  1.1, 2.8  $\pm$  1.9, and 4.1  $\pm$  3.3 ng m<sup>-3</sup>, respectively; Figure 4). The concentrations of the C5-alkene triols and MTLs exceeded that of 2-MGA. Generally, These isoprene-derived oxidation products are formed via acid-catalyzed ring-opening reactions and isomerization of isoprene epoxydiols (IEPOX), a reactive intermediate produced by the gas-phase oxidation of biogenic isoprene emitted by vegetation (Surratt et al., 2006 and 2010; Fu et al., 2010 and 2014; Shrivastava et al., 2017). Throughout the sampling period, a strong linear correlation was observed between the MTLs and C5-alkene triols (R<sup>2</sup> = 0.82, P < 0.01), indicating their

similar sources. Both species are sensitive to aerosol acidity and NO<sub>x</sub> levels, with lower aerosol pH and reduced NO<sub>x</sub> concentrations favoring their formation (Surratt et al., 2010; Lin et al., 2013). Nevertheless, certain differences were observed in the formation processes of C5-alkene triols and MTLs. For example, some studies have reported that, compared to MTLs, C5-alkene triols are more susceptible to degradation under high temperature and intense solar radiation, resulting in reduced C5/MTLs ratios in summer versus winter (Yee et al., 2020; Haque et al., 2023; Zhang et al., 2024). A similar seasonal decrease in the C5/MTLs ratio is observed in summer in our dataset (Figure S6a). C5-alkene triols and MTLs are believed to form via isoprene oxidation under low-NO<sub>x</sub> conditions. Contrarily, high concentrations of NO<sub>x</sub> favor further isoprene oxidation to yield 2-MGA (Lin et al., 2013; Nguyen et al., 2015). Here, the 2-MGA/MTL ratios in winter exceeded those observed in other seasons (Figure S6b), indicating that elevated NO<sub>x</sub> concentrations in winter (Figure S2) may enhance 2-MGA formation. In MTLs, 2-methylthreitol and 2-methylerythritol (MTL1 and MTL2) exhibited a significant linear correlation ( $R^2 = 0.68$ , P < 0.01), indicating that they may originate from similar sources and/or share similar formation pathways. The ratio of MTL2 to MTLs (MTL2/MTL ratio) can reflect the transformation pathways of MTLs. The ratio of MTL2/MTLs = 0.35, 0.61, 0.76, and 0.90 corresponded to isoprene secondary transformation from biogenic sources, OH-rich conditions (low NO<sub>x</sub>), NO<sub>x</sub>-rich conditions, and liquid-phase oxidation by H<sub>2</sub>O<sub>2</sub>, respectively (Kleindienst et al., 2009; Nozière et al., 2011). The results showed that the MTL2/MTL values in spring  $(0.64 \pm 0.12)$  and summer  $(0.59 \pm 0.11)$  were relatively low and closer to the values for biogenic sources and OH-rich secondary transformation. However, the values in autumn and  $(0.66 \pm 0.10)$  winter  $(0.69 \pm 0.06)$  were relatively high, approaching those for NO<sub>x</sub>-rich secondary transformation and liquid-phase oxidation by H<sub>2</sub>O<sub>2</sub> (Figure S6c). This indicates that in spring and summer, MTLs were more likely derived from biogenic sources and OH-rich secondary transformation, whereas in autumn and winter, a shift was observed toward NO<sub>x</sub>-rich secondary transformations and liquid-phase oxidation by H<sub>2</sub>O<sub>2</sub>. This relatively high C5/MTL, 2-MGA/MTL, or MTL2/MTL ratio observed during the cold season compared to that in the warm season is also commonly reported in urban environments across China, including Beijing (Liu et al., 2023), Tianjin (Wang et al., 2019; Fan et al., 2019), Nanjing (Yang et al., 2022), Shanghai (Yang et al., 2022), and Guangzhou (Yuan et al., 2018). Notably, the C5-alkene triols detected in our study predominantly exist as double-bonded "triol" compounds, including cis-2-methyl-1,3,4-trihydroxy-1-

430

431

432

433

434

435

436

437

438

439

440

441

442

443

444

445

446

447

448

449

450

451

452

453

454

455

456

butene, 3-methyl-2,3,4-trihydroxy-1-butene, and trans-2-methyl-1,3,4-trihydroxy-1-butene. In fact, acidcatalyzed ring-opening reactions and isomerization of particle-phase IEPOX can also produce various "diol" compounds, which typically exist as cyclic structures, such as trans-3-methyltetrahydrofuran-3,4-diol and cis-3-methyltetrahydrofuran-3,4-diol. These "diols" are also important components of C5-alkene triols (Li et al., 2013; Frauenheim et al., 2022). Recent work, however, indicates that C5-alkene triols detected via GC-MS are unlikely to originate solely from the acid-catalyzed ring-opening reactions and isomerization of IEPOX; instead, they may largely be artifacts produced by thermal decomposition during GC-MS analysis, with roughly 90% of the detected "triol" signal attributable to such artifacts (Frauenheim et al., 2022). If such artifacts indeed exist in the GC-MS measurements, it implies that the C5-alkene triol levels reported in our results are overestimated, potentially leading to an overall overestimation of isoprene-derived SOA tracers by approximately 30%. Despite the potential artifact issue in GC-MS detection, the contribution of C5-alkene triols to SOA should not be underestimated. These compounds are semi-volatile compounds that can volatilize back into the atmosphere from the particle phase, where they may undergo further oxidation by OH radicals. This oxidation process can significantly influence both the mass and composition of SOAs (Frauenheim et al., 2022 and 2024). Monoterpenes represent a crucial component of BVOC emissions, accounting for ~11% of the annual emissions, with an annual emission of 110 Tg C (Guenther et al., 1995). Here, we identified four oxidation products of monoterpene: pinonic acid (PNA); pinic acid (PA); 3-methyl-1,2,3-butanetricarboxylic acid (MBTCA); and 3-hydroxyglutaric acid (3-HGA), at concentrations of  $1.7 \pm 1.0$ ,  $1.5 \pm 0.9$ ,  $0.8 \pm 0.6$ , and  $0.8 \pm$ 0.5 ng m<sup>-3</sup>, respectively (Figure 4). The concentrations of PNA and PA exceeded those of MBTCA and 3-HGA. PNA and PA are produced via the oxidation of α/β-pinene via reactions with O<sub>3</sub> and OH radicals, and the  $\alpha/\beta$ -pinene detected in the aerosol samples is primarily derived from biomass burning and higher plant release (Hallquist et al., 2009; Eddingsaas et al., 2012; Zhang et al., 2015; Iyer et al., 2021). The predominance of PNA over PA is attributable to its relatively high vapor pressure, consistent with previous findings (Fu et al., 2008 and 2010). PNA and PA are recognized as first-generation oxidation products of  $\alpha$ -/ $\beta$ -pinene, whereas MBTCA represents a second-generation oxidation product formed via the further photooxidation of PNA and PA with OH radicals. The relative concentrations of such first- and second-generation oxidation products

457

458

459

460

461

462

463

464

465

466

467

468

469

470

471

472

473

474

475

476

477

478

479

480

481

482

483

(M/P) reflect the oxidation degree and aging status of monoterpene compounds (Ding et al., 2014). Here, the M/P values were higher in spring  $(0.25 \pm 0.11)$  and summer  $(0.32 \pm 0.10)$  than in autumn  $(0.16 \pm 0.09)$  and winter (0.24  $\pm$  0.10). This suggests that higher temperatures and/or stronger radiation in spring and summer promoted the oxidation of monoterpene compounds (Figure S6d). The formation of 3-HGA is considered to occur via a ring-opening mechanism, probably linked to heterogeneous reactions of monoterpenes with irradiation in NO<sub>x</sub>-rich environments (Jaoui et al., 2005; Claeys et al., 2007). The ratio of MBTCA to 3-HGA (MBTCA/3-HGA) can be employed to distinguish monoterpenes as the secondary transformation of  $\alpha$ -pinene yields MBTCA at significantly higher rates relative to 3-HGA compared with β-pinene (Jaoui et al., 2005). Here, the annual MBTCA/3-HGA value was 1.18 ± 0.65 (Figure S6e), close to those observed in urban environments in the United States (0.81  $\pm$  0.32) and other cities in China (0.68  $\pm$  0.65) (Lewandowski et al., 2013; Ding et al., 2014). This suggests that monoterpenes in these urban environments have similar sources. The MBTCA/3-HGA value was higher in spring  $(1.31 \pm 0.66)$  and summer  $(1.45 \pm 0.70)$  than in autumn (1.09 $\pm$  0.72) and winter (0.88  $\pm$  0.32) (Figure S6e). This suggests that the contribution of  $\alpha$ -pinene to monoterpene was higher in spring and summer than in autumn and winter. This phenomenon can be attributed to the association of 3-HGA formation with NO<sub>x</sub>-rich environments, where the relatively high NO<sub>x</sub> concentrations in autumn and winter (Figure S2) may enhance 3-HGA production. The ratio of the total isoprene to monoterpene oxidation products (Iso/Pine) was lower in autumn and winter than in summer (Figure S6f). This pattern is also commonly observed in other urban environments of China, suggesting that the higher temperatures in summer favored isoprene release (Li et al., 2018; Fan et al., 2020; Liu et al., 2023).

484

485

486

487

488

489

490

491

492

493

494

495

496

497

498

499

500

501

502

503

504

505

506

507

508

509

510

BVOC emissions include a class of sesquiterpene compounds, among which  $\beta$ -caryophyllene is the most abundant and frequently reported (Ding et al., 2014; Fan et al., 2020).  $\beta$ -caryophyllinic acid, a product of the ozonolysis or photooxidation of  $\beta$ -caryophyllene, predominantly originates from biomass burning and natural plant emissions, including those from pine and birch trees (Helmig et al., 2006; Duhl et al., 2008). Here,  $\beta$ -caryophyllinic acid was detected at a concentration of 2.7  $\pm$  1.9 ng m<sup>-3</sup>. The  $\beta$ -caryophyllinic acid concentrations in autumn (3.2  $\pm$  1.8 ng m<sup>-3</sup>) and winter (4.6  $\pm$  1.6 ng m<sup>-3</sup>) exceeded those observed in spring (1.5  $\pm$  0.7 ng m<sup>-3</sup>) and summer (1.1  $\pm$  0.5 ng m<sup>-3</sup>) (Figure 4). The higher concentrations of caryophyllinic acid in autumn and winter may be associated with increased biomass burning and subsequent secondary

transformation of  $\beta$ -caryophyllene. During the sampling period, a significant positive linear correlation was observed between  $\beta$ -caryophyllinic acid and levoglucosan, supporting this inference ( $R^2 = 0.66$ , P < 0.01).

## 3.4.2 Anthropogenic SOA tracers

511

512

513

514

515

516

517

518

519

520

521

522

523

524

525

526

527

528

529

530

531

532

533

534

535

536

537

Anthropogenic SOA tracers include hydroxy and aromatic acids, which primarily originate from the secondary transformation of AVOCs. Although global AVOC emissions are relatively modest at 110 Tg C yr<sup>-1</sup> (Piccot et al., 1992) compared with BVOC emissions, which reach 1,150 Tg C yr<sup>-1</sup> (Guenther et al., 1995), the contribution of anthropogenic sources to SOA is frequently more pronounced in urban environments because of the impact of human activities (von Schneidemesser et al., 2010; Ding et al., 2012; Li et al., 2019). AVOC emissions in urban settings can enhance BVOC oxidation, promoting SOA formation (Carlton et al., 2010; Hoyle et al., 2011). Here, we identified two primary anthropogenic SOA tracers, 2,3-dihydroxy-4oxopentanoic acid (DHOPA) and phthalic acid, at concentrations of 1.7  $\pm$  1.1 and 6.4  $\pm$  4.1 ng m<sup>-3</sup>, respectively (Figures 3 and 4). DHOPA and phthalic acid are recognized as important markers for anthropogenic SOAs, produced via the oxidation of toluene and PAHs, such as naphthalene (Kawamura and Ikushima, 1993; Kleindienst et al., 2007 and 2012). Their concentrations were higher in autumn and winter than in spring and summer (Figures 3 and 4). This indicated a marked increase in the contribution of anthropogenic sources to SOA during the cold months. As typical anthropogenic SOA tracers, DHOPA and phthalic acid have been reported to exhibit significantly higher concentrations in urban areas than in suburban and remote regions, with higher levels in the cold season than in the warm season in China (Ding et al., 2014; Fan et al., 2019; Yang et al., 2022). SOAs in urban environments and in the cold season in China are more strongly influenced by anthropogenic emissions, such as those from fossil fuel combustion and biomass burning (Ding et al., 2012; Yuan et al., 2018; Fan et al., 2019).

#### 3.5 Source apportionment of OC and aerosol

Employing the CMB model and tracer-based approach, we quantified the contributions of POC and SOC to the total OC (Figure 5). The results showed that the POC and SOC concentrations were  $3.66 \pm 2.47$  and  $0.50 \pm 0.32$  µg m<sup>-3</sup> (Figures 5a–5c), accounting for  $57.66\% \pm 18.35\%$  and  $8.25\% \pm 3.23\%$  of the measured OC, respectively (Figure 5f). Our results indicate that POC continues to be the main contributor to OC. These results were within the reported ranges of POC (5%–76%) and SOC (3%–56%) (Stone et al., 2009; Guo et al.,

2012; Fan et al., 2020; Xu et al., 2021; Haque et al., 2023). Notably, anthropogenic sources, including biomass burning, coal combustion, motor vehicle emissions, and cooking, contributed the majority of POC  $(3.35 \pm 2.38)$  $\mu g m^{-3}$ , accounting for  $88.93\% \pm 6.88\%$ ). Natural sources, such as plant debris and fungal spores, contributed relatively little  $(0.32 \pm 0.17 \text{ µg m}^{-3})$ , accounting for  $11.07\% \pm 6.88\%$ ). For SOC, anthropogenic contributions  $(0.33 \pm 0.25 \,\mu \text{g m}^{-3})$ , accounting for  $60.67\% \pm 21.29\%$ , including toluene and naphthalene, exceeded biogenic contributions (0.17  $\pm$  0.09 µg m<sup>-3</sup>, accounting for 39.33%  $\pm$  21.15%), which included isoprene,  $\alpha/\beta$ -pinene, and β-caryophyllene. The relative abundances of anthropogenic POC and SOC were higher in autumn and winter, whereas biogenic POC and SOC exhibited greater relative abundances during spring and summer (Figures 5d-5f). These results underscore the significant influence of biogenic emissions during the warm months, whereas anthropogenic emissions exert a pronounced effect during the cold months. This situation is primarily attributed to the elevated temperatures, and increased solar radiation during the warm months facilitates VOC release from vegetation, thereby promoting biogenic POC emissions and SOC formation. Contrarily, the rise in anthropogenic POC emissions during the cold months fosters the development of anthropogenic SOC in the atmosphere. During winter, including both pollution episodes (Winter-P) and the remainder period (Winter-R), the contribution proportions of three main anthropogenic POC sources (biomass burning, coal combustion, and vehicle exhaust, 55%-62%) and anthropogenic SOC precursors (toluene and naphthalene, 6%-7%) were consistently higher than the annual averages (40% for these anthropogenic POC and 5% for anthropogenic SOC) (Figure 5f). This trend was even more pronounced during individual pollution episodes (Figure S7), with these anthropogenic POC contributions reaching 51%-71% and anthropogenic SOC contributions increasing to 6%-8% (Figure S7f). These findings suggest that POC from biomass burning, coal combustion, and vehicle exhaust, along with SOC originating from toluene and naphthalene, may be key drivers of wintertime organic aerosol pollution. The fraction of OC that remains unexplained by the CMB model and tracer-based methods and is therefore

538

539

540

541

542

543

544

545

546

547

548

549

550

551

552

553

554

555

556

557

558

559

560

561

562

563

564

classified as "other OC". This component is defined as the difference between measured OC and the summed contributions of POC and SOC from all apportioned sources estimated by the CMB model and tracer approaches. On average, other OC accounts for ~34% of measured OC (Figures. 5c, 5f). The presence of other OC likely reflects limitations in source identification: some OC forms (e.g., liquid-phase OC or aged primary

OC) are difficult to capture with either the CMB model or tracer techniques (Ding et al., 2014; Fan et al., 2019; Wu et al., 2020; Xu et al., 2021). Although absolute concentrations of other OC are lower in spring and summer than in autumn and winter, its fractional contribution shows the opposite seasonal pattern—about 45%-50% in spring and summer versus 12%-29% in autumn and winter (Figures. 5c, 5f). Similar patterns have been reported elsewhere in other citie of China, e.g., Beijing, where estimated concentrations of other OC are higher in winter but its proportion is greater in summer (~44% vs. 22-25% in winter) (Wang et al., 2009; Wu et al., 2020; Xu et al., 2021). Previous studies indicate that this "other OC" is likely dominated by SOC (Guo et al., 2012; Wu et al., 2020; Xu et al., 2021). To assess whether other OC is predominantly primary or secondary, we used an EC-based method to estimate total POC and SOC; unlike tracer methods, the EC approach simply partitions OC into POC and SOC and therefore can include unapportioned components. Accordingly, the POC calculated via EC-based method minus the POC calculated via CMB model yields the "other POC" (unapportioned POC), and similarly, SOC calculated via EC-based method minus the tracerbased SOC yields the "other SOC" (Figure. S8). Our results show that, across all four seasons, the concentration of other SOC exceeds that of other POC (Figures, S8a, S8b), indicating that these unidentified other OC components are likely predominantly SOC. The concentration of other SOC is substantially higher in autumn and winter—especially during pollution periods in winter—highlighting the critical role of SOC in aerosol pollution during these seasons (Figures. S8c, S8d). Conversely, the proportion of other SOC during summer is the highest among all seasons (around 32%) (Figure. S8b), suggesting that elevated temperatures and intense radiation during summer enhance SOC formation efficiency (Wu et al., 2020; Xu et al., 2021). Although the other SOC fraction exceeds other POC, EC-based estimates of total SOC remain smaller than total POC in all seasons. Similarly, SOC estimated by the tracer method is markedly lower than POC apportioned by the CMB model. These results together indicate that primary emissions play a significant role in urban OC pollution, with substantial POC contributions forming the basis for elevated OC concentrations. However, the influence of SOC should not be overlooked. Numerous studies have shown that even minor increases in SOC during winter pollution episodes can exacerbate OA pollution (Li et al., 2019; Xu et al., 2021; Haque et al., 2023).

565

566

567

568

569

570

571

572

573

574

575

576

577

578

579

580

581

582

583

584

585

586

587

588

589

590

591

Using the CMB model and tracer-based methods, we also quantified the contributions of POA and SOA to

PM<sub>2.5</sub> (Figure S9). The findings indicated that POA and SOA contributed  $6.86 \pm 4.55$  and  $1.02 \pm 0.63$  µg m<sup>-3</sup>, accounting for  $22.84\% \pm 9.71\%$  and  $3.47\% \pm 1.41\%$  of the observed PM<sub>2.5</sub> mass in Nanchang, respectively. The anthropogenic POA ( $6.26 \pm 4.37$  µg m<sup>-3</sup>, accounting for  $89.38\% \pm 8.26\%$ ) and SOA ( $0.65 \pm 0.48$  µg m<sup>-3</sup>, accounting for  $58.79\% \pm 21.30\%$ ) exceeded the natural POA ( $0.60 \pm 0.33$  µg m<sup>-3</sup>, accounting for  $10.34\% \pm 6.83\%$ ) and SOA ( $0.37 \pm 0.20$  µg m<sup>-3</sup>, accounting for  $41.21\% \pm 21.30\%$ ), respectively. The POA and SOA exhibited patterns analogous to those of POC and SOC, with greater contributions recorded in autumn and winter compared with spring and summer.

592

593

594

595

596

597

598

599

600

601

602

603

604

605

606

607

608

609

610

611

612

613

614

615

616

617

618

The calculation of POC and SOC contributions based on the CMB model and tracer-based method inherently involves uncertainties. For the CMB model, a primary source of uncertainty is the variability of tracer mass fractions within OC (foc) from the same primary emission sources across various observational studies. For example, reported levoglucosan/OC fractions range from 12% (Andreae, et al., 2001, 2019) to 13% (Zheng et al., 2002) and 16% (Fine et al., 2004), whereas the local source profile we reference suggests 8.3% (Zhang et al., 2007). Since recent, site-specific emission data are often unavailable, the choice of source profile and corresponding f<sub>OC</sub> values can strongly influence apportionment outcomes. Secondly, a fundamental assumption of the CMB model is that the selected markers representing various sources remain stable during atmospheric transport and do not undergo significant chemical transformation. However, truly conservative species are rare. For example, levoglucosan, commonly used as a biomass-burning marker and generally considered relatively stable (Wan et al., 2021), has nonetheless been shown to decrease during long-range transport through wet and dry deposition (Fu et al., 2011) and by photodegradation (Holmes and Petrucci, 2006; Stohl et al., 2007; Hoffmann et al., 2010). Analogous loss or alteration of other source tracers can bias CMB results, tending to underestimate contributions from sources whose markers are degraded or removed during transport. For tracer-based methods, the appropriateness of the selected f<sub>SOC</sub> and f<sub>SOA</sub> values is also crucial to the accuracy of the results. Compared with primary source profiles, direct observational information on secondary source profiles is sparse. This paucity reflects the experimental difficulty of reproducing atmospheric oxidation and photochemical ageing under representative light and precursor conditions in laboratory or chamber systems. Most studies employing tracer-based methods to estimate SOC and SOA contributions have relied on f<sub>SOC</sub> and f<sub>SOA</sub> values reported by Kleindienst et al. (2007, 2012), which are now

relatively dated. SOC and SOA formation are influenced not only by oxidants and sunlight but also by factors such as relative humidity, precursor concentrations, NO<sub>x</sub> levels, and other ambient variables. The chamber conditions cannot fully reproduce the complexity of real atmospheres, leading to inevitable discrepancies in f<sub>SOC</sub> and f<sub>SOA</sub> values between chamber-derived results and ambient air (Fu et al., 2009; Guo et al., 2012; Ding et al., 2012 and 2014; Haque et al., 2023). Additionally, the f<sub>SOC</sub> and f<sub>SOA</sub> values used were average, and their inherent standard deviations could result in deviations of 21% to 48% in the calculated SOC contributions from different sources (Kleindienst et al. 2007 and 2012). Despite the inherent uncertainties associated with both the CMB model and tracer-based method, these approaches remain convenient tools for estimating the contributions of various POC and SOC, yielding relatively reasonable results (Stone et al., 2009; Ding et al., 2012 and 2014; Al-Naiema et al., 2017; Ren et al., 2021; Xu et al., 2021; Haque et al., 2023). However, further efforts are needed to reduce these uncertainties. One critical step will be to conduct more extensive, sitespecific observational studies of different types of primary and secondary emission sources. Such data are essential for identifying representative tracers within different sources and accurately determining their mass fractions in OC and OAs. Additionally, when f<sub>SOC</sub> and f<sub>SOA</sub> values are applied in both CMB model and tracerbased calculations, using the most recent, locally relevant emission source profile to minimize uncertainties is advisable.

#### 3.6 Characteristics of OAs during winter pollution

From an annual timescale perspective, anthropogenic POC and SOC are synchronous with the measured OC and observed  $PM_{2.5}$  mass (Figure S10). Correlation analysis revealed that anthropogenic POC (biomass burning, coal combustion, and vehicle exhaust) and SOC exhibited a significant positive correlation (r = 0.72– 0.84, P < 0.01) with the measured OC (Figure 6a). Redundancy analysis revealed that anthropogenic POC and SOC significantly contributed (54%–65%, P < 0.01) to the variations in OC concentration (Figure 6a). This suggests that anthropogenic OC and SOC are important factors influencing changes in the OC and  $PM_{2.5}$  mass throughout the sampling period. Variations in POC, SOC, OC, and  $PM_{2.5}$  mass were associated with specific meteorological conditions and gaseous pollutant concentrations. For instance, high POC, SOC, OC, and  $PM_{2.5}$  concentrations corresponded to elevated atmospheric pressure, reduced precipitation, and increased  $PNO_2$  concentrations (Figure S2). This suggests that meteorological conditions and gaseous pollutant concentrations

could also influence POC, SOC, OC, and PM<sub>2.5</sub> mass.

However, winter presents a different scenario. Regardless of whether it is during the winter pollution periods or other times in winter, POC did not maintain good consistency with the changes in the total OC content and  $PM_{2.5}$  mass, whereas SOC remained synchronized with their variations (Figure S11). This phenomenon is particularly pronounced during individual pollution episodes in winter (Figure S11). Correlation and redundancy analyses further revealed that source-specific SOC, derived using the tracer methods, and the total SOC, calculated using the EC-based method, exhibited significant positive correlations with the measured OC (r > 0.6, P < 0.05) and significantly contributed (> 40%, P < 0.05) to their variations in entire winter pollution periods and individual pollution episodes (Figures 6b and 6d–6l). Given the relatively small number of nonpolluted days in winter and their scattered distribution across different dates, the correlations and contribution levels were not as evident during the remainder of the winter season (Figures 6c). These findings indicate that on shorter timescales, particularly during brief PM pollution episodes lasting several days, SOC was a critical factor influencing the total OC content and  $PM_{2.5}$  mass.

The increased SOC concentration may be associated with elevated temperatures and NO<sub>x</sub> concentrations during winter pollution episodes. This inference was supported by a significant linear positive correlation between temperature, NO<sub>2</sub> concentrations, and SOC concentrations observed during entire winter pollution periods and individual pollution episodes (Figures 7b and 7d–7l). Before conducting linear correlation analyses, the Shapiro-Wilk test was used to assess the normality of the data, and linear correlations were conducted only for datasets significantly conforming to a normal distribution (p > 0.05). An increase in short-term solar radiation intensity and oxidant levels have been shown to accelerate SOC formation (Fry et al., 2009; Ng et al., 2017; Li et al., 2018; Ren et al., 2019). Nevertheless, the contribution of POC should not be underestimated as its levels remained relatively high throughout the winter. This elevated POC concentration can also promote SOC transformation (Weber et al., 2007; Carlton et al., 2010; Hoyle et al., 2011; Srivastava et al., 2022). Outside pollution periods in winter, variations in temperature and NO<sub>2</sub> concentrations are minimal, which limits their promoting effect on SOC concentration increases (Figure 7c). Additionally, we analyzed the linear correlations between other meteorological factors and SOC. In particular, we examined the relations between wind speed, relative humidity, and SOC (Figure S12). The results indicated that no clear relation

existed between wind speed and SOC. Although relative humidity showed some linear association with SOC during a few isolated pollution episodes, this relation was weak, with relatively large P-values and lacking statistical significance. These findings suggest that temperature and NO<sub>2</sub> concentrations are likely the main meteorological and oxidative factors driving the increase of SOC during winter pollution periods in the Nanchang region.

#### 4 Conclusions

We investigated the composition and concentration of major polar organic compounds in  $PM_{2.5}$  samples collected over a year in Nanchang, Central China. The results revealed relatively high concentrations of FAs, fatty alcohols, and saccharides, whereas lignin, resin products, sterols, glycerol, hydroxy acids, and aromatic acids were detected at low levels.

The study findings indicate that the organic components in the PM<sub>2.5</sub> of Nanchang are predominantly derived from anthropogenic and natural sources. Anthropogenic sources were the primary contributors to OC and OA, and primary sources contributed more than secondary sources. Throughout the sampling period, we observed that the anthropogenic contributions significantly increased during autumn and winter, whereas biogenic contributions increased in spring and summer.

This study highlights the critical role of anthropogenic POC and SOC in influencing atmospheric PM<sub>2.5</sub> pollution over an annual sampling period. During short-term pollution episodes in winter (lasting several days), the rapid secondary transformation emerged as the primary driver of OC increment and PM<sub>2.5</sub> pollution. Elevated primary emissions and favorable oxidation conditions, such as increased light intensity and NO<sub>x</sub> levels, were identified as key factors facilitating the rapid secondary transformation of OC during the winter pollution episodes.

The study findings underscore the necessity for targeted management strategies that consider primary and secondary anthropogenic emission sources across different seasons and pollution periods. Although the CMB model and tracer-based method provided preliminary insights into the OC and OA from diverse sources, the study encountered several inherent limitations. First, the primary emission source profiles employed in the CMB model exhibit variability across different studies and regions, making it challenging to establish standardized source characteristic parameters and potentially affecting the accuracy of source apportionment.

Second, the proportions of SOC tracers obtained from laboratory chamber experiments are influenced by various factors, and incorporating these proportions into tracer-based methods may introduce potential biases or uncertainties in the estimates. To address these issues, future research should prioritize comprehensive observational studies of primary emission sources to obtain high-resolution, region-specific emission data, thereby improving the applicability of source profiles. Combining field observations with laboratory simulations can also provide a more accurate characterization of secondary emissions, ultimately reducing the uncertainties associated with tracer-based estimates of SOC contributions.

**Data availability.** The dataset associated with this paper is available upon request from the corresponding author (xiaohuayun@sjtu.edu.cn).

**Competing interests.** The authors declare that they have no conflict of interest.

**Author contributions.** Huayun Xiao conceptualized and designed the research. Sampling was conducted by Zicong Li, and laboratory analyses were conducted by Wei Guo, Zicong Li, and Renguo Zhu. Data interpretation was supported by Zhongkui Zhou and Hongwei Xiao. The manuscript was primarily written by Wei Guo, with contributions and consultations from all other authors.

Acknowledgements. We thank Ziyue Zhang and Liqin Cheng for their help with sampling and laboratory work. This study was supported by the National Natural Science Foundation of China (grant number 41863002); the Jiangxi Provincial Natural Science Foundation (grant number 20242BAB25193); the Open Foundation of Jiangxi Province Key Laboratory of the Causes and Control of Atmospheric Pollution, East China University of Technology (grant number AE2209); and the Open Foundation of Yunnan Province Key Laboratory of Earth System Science, Yunnan University (grant number ESS2024002).

- 726 References
- 727 Al-Naiema, I. M., and Stone, E. A.: Evaluation of anthropogenic secondary organic aerosol tracers from
- 728 aromatic hydrocarbons, Atmos. Chem. Phys., 17, 2053–2065, https://doi.org/10.5194/acp-17-2053-2017,
- 729 2017.
- 730 An, Z. S., Huang, R. J., Zhang, R. Y., Tie, X. X., Li, G. H., Cao, J. J., Zhou, W. J., Shi, Z. G., Han, Y. M., Gu,
- 731 Z. L., and Ji, Y. M.: Severe haze in northern China: A synergy of anthropogenic emissions and atmospheric
- processes, Proc. Natl. Acad. Sci. U.S.A., 116, 8657–8666, https://doi.org/10.1073/pnas.1900125116, 2019.
- 733 Andreae, M. O., and Merlet, P.: Emission of trace gases and aerosols from biomass burning, Global
- 734 Biogeochem. Cy., 15, 955–966, https://doi.org/10.1029/2000GB001382, 2001.
- Andreae, M. O.: Emission of trace gases and aerosols from biomass burning an updated assessment, Atmos.
- 736 Chem. Phys., 19, 8523–8546, https://doi.org/10.5194/acp-19-8523-2019, 2019.
- Bauer, H., Claeys, M., Vermeylen, R., Schueller, E., Weinke, G., Berger, A., and Puxbaum, H.: Arabitol and
- mannitol as tracers for the quantification of airborne fungal spores, Atmos. Environ., 42, 588-593,
- 739 https://doi.org/10.1016/j.atmosenv.2007.10.013, 2008.
- Bauer, H., Kasper-Giebl, A., Zibuschka, F., Hitzenberger, R., Kraus, G. F., and Puxbaum, H.: Determination
- 741 of the Carbon Content of Airborne Fungal Spores, Anal. Chem., 74, 91–95,
- 742 https://doi.org/10.1021/ac010331+, 2002.
- Cai, T., Zhang, Y., Fang, D., Shang, J., Zhang, Y., and Zhang, Y.: Chinese vehicle emissions characteristic
- testing with small sample size: Results and comparison, Atmos. Pollut. Res., 8, 154–163,
- 745 https://doi.org/10.1016/j.apr.2016.08.007, 2017.
- Cao, J. J., and Cui, L.: Current Status, Characteristics and Causes of Particulate Air Pollution in the Fenwei
- 747 Plain, China: A Review, J. Geophys.Res-Atmos., 126, e2020JD034472,
- 748 https://doi.org/10.1029/2020JD034472, 2021.
- 749 Cao, J. J, Xu, H. M, Xu, Q., Chen, B. H., and Kan, H. D.: Fine particulate matter constituents and
- cardiopulmonary mortality in a heavily polluted Chinese city, Environ. Health Perspect., 120, 373–378,
- 751 https://doi.org/10.1289/ehp.1103671, 2012.
- 752 Carlton, A. G., Pinder, R. W., Bhave, P. V., and Pouliot, G. A.: To What Extent Can Biogenic SOA be
- 753 Controlled?, Environ. Sci. Technol., 44, 3376–3380, https://doi.org/10.1021/es903506b, 2010.
- Castro, L. M., Pio, C. A., Harrison, R. M., and Smith, D. J. T.: Carbonaceous aerosol in urban and rural
- 755 European atmospheres: estimation of secondary organic carbon concentrations, Atmos. Environ., 33, 2771–
- 756 2781, https://doi.org/10.1016/S1352-2310(98)00331-8, 1999.

- 757 Chen, C. R., Zhang, H. X., Yan, W. J., Wu, N. N., Zhang, Q., and He, K. B.: Aerosol water content
- enhancement leads to changes in the major formation mechanisms of nitrate and secondary organic aerosols
- 759 in winter over the North China Plain, Environ. Pollut., 287, 117625,
- 760 https://doi.org/10.1016/j.envpol.2021.117625, 2021.
- 761 Chow, J. C., Watson, J. G., Chen, L. W. A., Chang, M. C. O., Robinson, N. F., Trimble, D., and Kohl, S.: The
- 762 IMPROVE\_A Temperature Protocol for Thermal/Optical Carbon Analysis: Maintaining Consistency with a
- 763 Long-Term Database, J. Air Waste Manage., 57, 1014–1023, https://doi.org/10.3155/1047-3289.57.9.1014,
- 764 2007.
- 765 Cheng, Y. B., Ma, Y. Q., and Hu, D.: Tracer-based source apportioning of atmospheric organic carbon and the
- influence of anthropogenic emissions on secondary organic aerosol formation in Hong Kong, Atmos. Chem.
- 767 Phys., 21, 10589–10608, https://doi.org/10.5194/acp-21-10589-2021, 2021.
- Claeys, M., Graham, B., Vas, G., Wang, W., Vermeylen, R., Pashynska, V., Cafmeyer, J., Guyon, P., Andreae,
- M. O., Artaxo, P., and Maenhaut, W.: Formation of Secondary Organic Aerosols Through Photooxidation
- of Isoprene, Science, 303, 1173–1176, https://doi.org/doi:10.1126/science.1092805, 2004.
- 771 Claeys, M., Szmigielski, R., Kourtchev, I., Van der Veken, P., Vermeylen, R., Maenhaut, W., Jaoui, M.,
- Kleindienst, T. E., Lewandowski, M., Offenberg, J. H., and Edney, E. O.: Hydroxydicarboxylic Acids:
- 773 Markers for Secondary Organic Aerosol from the Photooxidation of α-Pinene, Environ. Sci. Technol., 41,
- 774 1628–1634, https://doi.org/10.1021/es0620181, 2007.
- Ding, X., Wang, X. M., Gao, B., Fu, X. X., He, Q. F., Zhao, X. Y., Yu, J. Z., and Zheng, M.: Tracer-based
- estimation of secondary organic carbon in the Pearl River Delta, south China, J. Geophys. Res-Atmos., 117,
- 777 https://doi.org/10.1029/2011JD016596, 2012.
- 778 Ding, X., Wang, X. M., Xie, Z. Q., Zhang, Z., and Sun, L. G.: Impacts of Siberian Biomass Burning on
- Organic Aerosols over the North Pacific Ocean and the Arctic: Primary and Secondary Organic Tracers,
- 780 Environ. Sci. Technol., 47, 3149–3157, https://doi.org/10.1021/es3037093, 2013.
- Ding, X., He, Q. F., Shen, R. Q., Yu, Q. Q., and Wang, X. M.: Spatial distributions of secondary organic
- 782 aerosols from isoprene, monoterpenes, β-caryophyllene, and aromatics over China during summer, J.
- 783 Geophys. Res-Atmos., 119, 11877–811891, https://doi.org/10.1002/2014JD021748, 2014.
- Duhl, T. R., Helmig, D., and Guenther, A.: Sesquiterpene emissions from vegetation: a review, Biogeosciences,
- 785 5, 761–777, https://doi.org/10.5194/bg-5-761-2008, 2008.
- 786 Eddingsaas, N. C., Loza, C. L., Yee, L. D., Chan, M., Schilling, K. A., Chhabra, P. S., Seinfeld, J. H., and
- 787 Wennberg, P. O.: α-pinene photooxidation under controlled chemical conditions-Part 2: SOA yield and

- 788 composition in low- and high-NO<sub>x</sub> environments, Atmos. Chem. Phys., 12, 7413–7427,
- 789 https://doi.org/10.5194/acp-12-7413-2012, 2012.
- 790 Engling, G., He, J., Betha, R., and Balasubramanian, R.: Assessing the regional impact of indonesian biomass
- burning emissions based on organic molecular tracers and chemical mass balance modeling, Atmos. Chem.
- 792 Phys., 14, 8043–8054, https://doi.org/10.5194/acp-14-8043-2014, 2014.
- 793 Fabbri, D., Torri, C., Simoneit, B. R. T., Marynowski, L., Rushdi, A. I., and Fabiańska, M. J.: Levoglucosan
- and other cellulose and lignin markers in emissions from burning of Miocene lignites, Atmos. Environ., 43,
- 795 2286–2295, https://doi.org/10.1016/j.atmosenv.2009.01.030, 2009.
- 796 Fan, Y. B., Liu, C. Q., Li, L. J., Ren, L. J., Ren, H., Zhang, Z. M., Li, Q. K., Wang, S., Hu, W., Deng, J. J., Wu,
- 797 L. B., Zhong, S. J., Zhao, Y., Pavuluri, C. M., Li, X. D., Pan, X. L., Sun, Y. L., Wang, Z. F, Kawamura, K.,
- 798 Shi, Z. B., and Fu, P. Q.: Large contributions of biogenic and anthropogenic sources to fine organic
- aerosols in Tianjin, North China, Atmos. Chem. Phys., 20, 117–137, https://doi.org/10.5194/acp-20-117-
- 800 2020, 2020.
- Fine, P. M., Cass, G. R., and Simoneit, B. R. T.: Chemical Characterization of Fine Particle Emissions from
- the Fireplace Combustion of Wood Types Grown in the Midwestern and Western United States, Environ.
- 803 Eng. Sci., 21, 387–409, https://doi.org/10.1089/109287504323067021, 2004.
- Frauenheim, M., Offenberg, J., Zhang, Z., Surratt, J. D., and Gold, A.: The C5-Alkene Triol Conundrum:
- Structural Characterization and Quantitation of Isoprene-Derived C<sub>5</sub>H<sub>10</sub>O<sub>3</sub> Reactive Uptake Products,
- 806 Environ. Sci. Tech. Let., 9, 829–836, https://doi.org/10.1021/acs.estlett.2c00548, 2022.
- 807 Frauenheim, M., Offenberg, J., Zhang, Z., Surratt, J. D., and Gold, A.: Chemical Composition of Secondary
- 808 Organic Aerosol Formed from the Oxidation of Semivolatile Isoprene Epoxydiol Isomerization Products,
- 809 Environ. Sci. Technol., 58, 22571–22582, https://doi.org/10.1021/acs.est.4c06850, 2024.
- 810 Fry, J. L., Kiendler-Scharr, A., Rollins, A. W., Wooldridge, P. J., Brown, S. S., Fuchs, H., Dub & W., Mensah,
- A., dal Maso, M., Tillmann, R., Dorn, H. P., Brauers, T., and Cohen, R. C.: Organic nitrate and secondary
- organic aerosol yield from NO<sub>3</sub> oxidation of β-pinene evaluated using a gas-phase kinetics/aerosol
- 813 partitioning model, Atmos. Chem. Phys., 9, 1431–1449, https://doi.org/10.5194/acp-9-1431-2009, 2009.
- 814 Fu, P. Q., Kawamura, K., Okuzawa, K., Aggarwal, S. G., Wang, G., Kanaya, Y., and Wang, Z.: Organic
- 815 molecular compositions and temporal variations of summertime mountain aerosols over Mt. Tai, North
- China Plain, J. Geophys. Res-Atmos., 113, https://doi.org/10.1029/2008JD009900, 2008.
- 817 Fu, P. Q., Kawamura, K., and Barrie, L. A.: Photochemical and other sources of organic compounds in the
- Canadian high arctic aerosol pollution during winter-spring, Environ. Sci. Technol., 43, 286–292,
- 819 https://doi.org/10.1021/es803046q, 2009.

- 820 Fu, P. Q., Kawamura, K., Pavuluri, C. M., Swaminathan, T., and Chen, J.: Molecular characterization of urban
- organic aerosol in tropical India: contributions of primary emissions and secondary photooxidation, Atmos.
- 822 Chem. Phys., 10, 2663–2689, https://doi.org/10, 2663-2689, 10.5194/acp-10-2663-2010, 2010.
- 823 Fu, P. Q, Kawamura, K., and Miura, K.: Molecular characterization of marine organic aerosols collected
- during a round-the-world cruise, J. Geophys. Res-Atmos., 116, https://doi.org/10.1029/2011JD015604,
- 825 2011.
- 826 Fu, P. Q., Kawamura, K., Kobayashi, M., and Simoneit, B. R. T.: Seasonal variations of sugars in atmospheric
- 827 particulate matter from Gosan, Jeju Island: Significant contributions of airborne pollen and Asian dust in
- spring, Atmos. Environ., 55, 234–239, https://doi.org/10.1016/j.atmosenv.2012.02.061, 2012.
- 829 Fu, P. Q., Kawamura, K., Chen, J., and Miyazaki, Y.: Secondary Production of Organic Aerosols from
- 830 Biogenic VOCs over Mt. Fuji, Japan, Environ. Sci. Technol., 48, 8491-8497,
- https://doi.org/10.1021/es500794d, 2014.
- Graham, B., Guyon, P., Taylor, P. E., Artaxo, P., Maenhaut, W., Glovsky, M. M., Flagan, R. C., and Andreae,
- M. O.: Organic compounds present in the natural Amazonian aerosol: Characterization by gas
- chromatography–mass spectrometry, J. Geophys. Res-Atmos., 108, https://doi.org/10.1029/2003JD003990,
- 835 2003.
- Guenther, A., Hewitt, C. N., Erickson, D., Fall, R., Geron, C., Graedel, T., Harley, P., Klinger, L., Lerdau, M.,
- Mckay, W. A., Pierce, T., Scholes, B., Steinbrecher, R., Tallamraju, R., Taylor, J., and Zimmerman, P.: A
- global model of natural volatile organic compound emissions, Res-Atmos., 100, 8873-8892,
- https://doi.org/10.1029/94JD02950, 1995.
- Guo, S., Hu, M., Guo, Q., Zhang, X., Zheng, M., Zheng, J., Chang, C. C., Schauer, J. J., and Zhang, R.:
- Primary Sources and Secondary Formation of Organic Aerosols in Beijing, China, Environ. Sci. Technol.,
- 842 46, 9846–9853, 10.1021/es2042564, 2012.
- 843 Guo, W., Li, Z. C., Zhang, Z. Y., Zhu, R. G., Xiao, H. W., and Xiao, H. Y.: Sources and influences of
- atmospheric nonpolar organic compounds in Nanchang, central China: Full-year monitoring with a focus
- on winter pollution episodes, Sci. Total Environ., 912, 169216,
- 846 https://doi.org/10.1016/j.scitotenv.2023.169216, 2024a.
- 847 Guo, W., Zhang, Z. Y., Zhu, R. G., Li, Z. C., Liu, C., Xiao, H. W., and Xiao, H. Y.: Pollution characteristics,
- sources, and health risks of phthalate esters in ambient air: A daily continuous monitoring study in the
- 849 central Chinese city of Nanchang, Chemosphere, 353, 141564,
- https://doi.org/10.1016/j.chemosphere.2024.141564, 2024b.

- Hallquist, M., Wenger, J. C., Baltensperger, U., Rudich, Y., Simpson, D., Claeys, M., Dommen, J., Donahue,
- N. M., George, C., Goldstein, A. H., Hamilton, J. F., Herrmann, H., Hoffmann, T., Iinuma, Y., Jang, M.,
- Jenkin, M. E., Jimenez, J. L., Kiendler-Scharr, A., Maenhaut, W., McFiggans, G., Mentel, T. F., Monod, A.,
- Pr év ât, A. S. H., Seinfeld, J. H., Surratt, J. D., Szmigielski, R., and Wildt, J.: The formation, properties and
- impact of secondary organic aerosol: current and emerging issues, Atmos. Chem. Phys., 9, 5155–5236,
- 856 10.5194/acp-9-5155-2009, 2009.
- 857 Haque, M. M., Kawamura, K., Deshmukh, D. K., Fang, C., Song, W., Mengying, B., and Zhang, Y. L.:
- Characterization of organic aerosols from a Chinese megacity during winter: predominance of fossil fuel
- combustion, Atmos. Chem. Phys., 19, 5147–5164, 10.5194/acp-19-5147-2019, 2019.
- Haque, M. M., Zhang, Y., Bikkina, S., Lee, M., and Kawamura, K.: Regional heterogeneities in the emission
- of airborne primary sugar compounds and biogenic secondary organic aerosols in the East Asian outflow:
- evidence for coal combustion as a source of levoglucosan, Atmos. Chem. Phys., 22, 1373-1393,
- 863 10.5194/acp-22-1373-2022, 2022.
- Haque, M. M., Verma, S. K., Deshmukh, D. K., Kunwar, B., and Kawamura, K.: Seasonal characteristics of
- biogenic secondary organic aerosol tracers in a deciduous broadleaf forest in northern Japan, Chemosphere,
- 311, 136785, https://doi.org/10.1016/j.chemosphere.2022.136785, 2023.
- He, L. Y., Hu, M., Huang, X. F., Yu, B. D., Zhang, Y. H., and Liu, D. Q.: Measurement of emissions of fine
- particulate organic matter from Chinese cooking, Atmos. Environ., 38, 6557–6564,
- https://doi.org/10.1016/j.atmosenv.2004.08.034, 2004.
- He, L. Y., Hu, M., Huang, X. F., Zhang, Y. H., and Tang, X. Y.: Seasonal pollution characteristics of organic
- compounds in atmospheric fine particles in Beijing, Sci. Total Environ., 359, 167–176,
- 872 https://doi.org/10.1016/j.scitotenv.2005.05.044, 2006.
- Helmig, D., Ortega, J., Guenther, A., Herrick, J. D., and Geron, C.: Sesquiterpene emissions from loblolly pine
- and their potential contribution to biogenic aerosol formation in the Southeastern US, Atmos. Environ., 40,
- 875 4150–4157, https://doi.org/10.1016/j.atmosenv.2006.02.035, 2006.
- 876 Holmes, B. J., and Petrucci, G. A.: Water-soluble oligomer formation from acid-catalyzed reactions of
- levoglucosan in proxies of atmospheric aqueous aerosols, Environ. Sci. Technol., 40, 4983–4989,
- 878 https://doi.org/10.1021/es060646c, 2006.
- Hoffmann, D., Tilgner, A., Iinuma, Y., and Herrmann, H.: Atmospheric stability of levoglucosan: a detailed
- laboratory and modeling study, Environ. Sci. Technol., 44, 694–699, https://doi.org/10.1021/es902476f,
- 881 2010.

- Hoyle, C. R., Boy, M., Donahue, N. M., Fry, J. L., Glasius, M., Guenther, A., Hallar, A. G., Huff Hartz, K.,
- Petters, M. D., Pet ä ä, T., Rosenoern, T., and Sullivan, A. P.: A review of the anthropogenic influence on
- biogenic secondary organic aerosol, Atmos. Chem. Phys., 11, 321–343, https://doi.org/10.5194/acp-11-321-
- 885 2011, 2011.
- Huang, R. J., Zhang, Y., Bozzetti, C., Ho, K. F., Cao, J. J., Han, Y., Daellenbach, K. R., Slowik, J. G., Platt, S.
- 887 M., Canonaco, F., Zotter, P., Wolf, R., Pieber, S. M., Bruns, E. A., Crippa, M., Ciarelli, G., Piazzalunga, A.,
- 888 Schwikowski, M., Abbaszade, G., Schnelle-Kreis, J., Zimmermann, R., An, Z., Szidat, S., Baltensperger,
- 889 U., El Haddad, I., and Prevot, A. S.: High secondary aerosol contribution to particulate pollution during
- haze events in China, Nature, 514, 218–222, https://doi.org/10.1038/nature13774, 2014.
- Huang, Y., Shen, H., Chen, Y., Zhong, Q., Chen, H., Wang, R., Shen, G., Liu, J., Li, B., and Tao, S.: Global
- organic carbon emissions from primary sources from 1960 to 2009, Atmos. Environ., 122, 505–512,
- 893 https://doi.org/10.1016/j.atmosenv.2015.10.017, 2015.
- Huebert, B., Bates, T., Russell, P., Shi, G., Kim, Y., Kawamura, K., Carmichael, G., and Nakajima, T.: An
- 895 overview of ACE-Asia: Strategies for quantifying the relationships between Asian aerosols and their
- 896 climatic impacts, J. Geophys. Res-Atmos., https://doi.org/108, 10.1029/2003JD003550, 2003.
- 897 Iinuma, Y., Brüggemann, E., Gnauk, T., Müller, K., Andreae, M. O., Helas, G., Parmar, R., and Herrmann, H.:
- 898 Source characterization of biomass burning particles: The combustion of selected European conifers,
- 899 African hardwood, savanna grass, and German and Indonesian peat, J. Geophys. Res-Atmos., 112,
- 900 https://doi.org/10.1029/2006JD007120, 2007.
- 901 Iyer, S., Rissanen, M. P., Valiev, R., Barua, S., Krechmer, J. E., Thornton, J., Ehn, M., and Kurtén, T.:
- 902 Molecular mechanism for rapid autoxidation in α-pinene ozonolysis, Nat. Commun., 12, 878,
- 903 10.1038/s41467-021-21172-w, 2021.
- Jaoui, M., Kleindienst, T. E., Lewandowski, M., Offenberg, J. H., and Edney, E. O.: Identification and
- Quantification of Aerosol Polar Oxygenated Compounds Bearing Carboxylic or Hydroxyl Groups. 2.
- 906 Organic Tracer Compounds from Monoterpenes, Environ. Sci. Technol., 39, 5661-5673,
- 907 10.1021/es048111b, 2005.
- 908 Jaoui, M., Szmigielski, R., Nestorowicz, K., Kolodziejczyk, A., Sarang, K., Rudzinski, K. J., Konopka, A.,
- 909 Bulska, E., Lewandowski, M., and Kleindienst, T. E.: Organic Hydroxy Acids as Highly Oxygenated
- 910 Molecular (HOM) Tracers for Aged Isoprene Aerosol, Environ. Sci. Technol., 53, 14516–14527,
- 911 10.1021/acs.est.9b05075, 2019.
- 912 Kanakidou, M., Seinfeld, J. H., Pandis, S. N., Barnes, I., Dentener, F. J., Facchini, M. C., Van Dingenen, R.,
- 913 Ervens, B., Nenes, A., Nielsen, C. J., Swietlicki, E., Putaud, J. P., Balkanski, Y., Fuzzi, S., Horth, J.,

- Moortgat, G. K., Winterhalter, R., Myhre, C. E. L., Tsigaridis, K., Vignati, E., Stephanou, E. G., and
- Wilson, J.: Organic aerosol and global climate modelling: a review, Atmos. Chem. Phys., 5, 1053–1123,
- 916 https://doi.org/10.5194/acp-5-1053-2005, 2005.
- 917 Kawamura, K., and Gagosian, R. B.: Implications of ω-oxocarboxylic acids in the remote marine atmosphere
- for photo-oxidation of unsaturated fatty acids, Nature, 325, 330–332, https://doi.org/10.1038/325330a0,
- 919 1987.
- 920 Kawamura, K., and Kaplan, I. R.: Motor exhaust emissions as a primary source for dicarboxylic acids in Los
- 921 Angeles ambient air, Environ. Sci. Technol., 21, 105–110, https://doi.org/10.1021/es00155a014, 1987.
- 922 Kawamura, K., and Ikushima, K.: Seasonal changes in the distribution of dicarboxylic acids in the urban
- 923 atmosphere, Environ. Sci. Technol., 27, 2227–2235, https://doi.org/10.1021/ES00047A033, 1993.
- 924 Kawamura, K., and Sakaguchi, F.: Molecular distributions of water soluble dicarboxylic acids in marine
- aerosols over the Pacific Ocean including tropics, J. Geophys. Res-Atmos., 104, 3501-3509,
- 926 https://doi.org/10.1029/1998JD100041, 1999.
- 927 Kawamura, K., Steinberg, S., and Kaplan, I. R.: Homologous series of C1–C10 monocarboxylic acids and C1–
- 928 C6 carbonyls in Los Angeles air and motor vehicle exhausts, Atmos. Environ., 34, 4175-4191,
- 929 https://doi.org/10.1016/S1352-2310(00)00212-0, 2000.
- 930 Kawamura, K., Ishimura, Y., and Yamazaki, K.: Four years' observations of terrestrial lipid class compounds
- 931 in marine aerosols from the western North Pacific, Global Biogeochem. Cy., 17, 1003,
- 932 https://doi.org/10.1029/2001GB001810, 2003.
- Kleindienst, T. E., Jaoui, M., Lewandowski, M., Offenberg, J. H., Lewis, C. W., Bhave, P. V., and Edney, E.
- O.: Estimates of the contributions of biogenic and anthropogenic hydrocarbons to secondary organic
- 935 aerosol at a southeastern US location, Atmos. Environ., 41, 8288-8300,
- 936 https://doi.org/10.1016/j.atmosenv.2007.06.045, 2007.
- 937 Kleindienst, T. E., Lewandowski, M., Offenberg, J. H., Jaoui, M., and Edney, E. O.: The formation of
- secondary organic aerosol from the isoprene <sup>+</sup>OH reaction in the absence of NO<sub>x</sub>, Atmos. Chem. Phys., 9,
- 939 6541–6558, 10.5194/acp-9-6541-2009, 2009.
- 940 Kleindienst, T.E., Jaoui, M., Lewandowski, M., Offenberg, J.H., and Docherty, K.S.: The formation of SOA
- and chemical tracer compounds from the photooxidation of naphthalene and its methyl analogs in the
- presence and absence of nitrogen oxides, Atmos. Chem. Phys., 12, 8711–8726 https://doi.org/10.5194/acp-
- 943 12-8711-2012, 2012.

- 844 Kunwar, B., and Kawamura, K.: One-year observations of carbonaceous and nitrogenous components and
- major ions in the aerosols from subtropical Okinawa Island, an outflow region of Asian dusts, Atmos.
- 946 Chem. Phys., 14, 1819–1836, https://doi.org/10.5194/acp-14-1819-2014, 2014.
- Lewandowski, M., Jaoui, M., Offenberg, J. H., Kleindienst, T. E., Edney, E. O., Sheesley, R. J., and Schauer, J.
- J.: Primary and secondary contributions to ambient PM in the midwestern United States, Environ. Sci.
- 949 Technol., 42, 3303–3309, https://doi.org/doi: 10.1021/es0720412, 2008.
- 950 Lewandowski, M., Piletic, I. R., Kleindienst, T. E., Offenberg, J. H., Beaver, M. R., Jaoui, M., Docherty, K. S.,
- 951 and Edney, E. O.: Secondary organic aerosol characterisation at field sites across the United States during
- 952 the spring-summer period, Int. J. Environ. An. Ch., 93, 1084–1103,
- 953 https://doi.org/10.1080/03067319.2013.803545, 2013.
- 954 Li, H., Cheng, J., Zhang, Q., Zheng, B., Zhang, Y., Zheng, G., and He, K.: Rapid transition in winter aerosol
- composition in Beijing from 2014 to 2017: response to clean air actions, Atmos. Chem. Phys., 19, 11485–
- 956 11499, https://doi.org/10.5194/acp-19-11485-2019, 2019.
- Li, J. J., Wang, G. H., Cao, J. J., Wang, X. M., and Zhang, R. J.: Observation of biogenic secondary organic
- aerosols in the atmosphere of a mountain site in central China: temperature and relative humidity effects,
- 959 Atmos. Chem. Phys., 13, 11535–11549, https://doi.org/10.5194/acp-13-11535-2013, 2013.
- 960 Li, J. J., Wang, G. H., Wu, C., Cao, C., Ren, Y.Q., Wang, J. Y., Li, J., Cao, J. J., Zeng, L. M., and Zhu, T.:
- 961 Characterization of isoprene-derived secondary organic aerosols at a rural site in North China Plain with
- implications for anthropogenic pollution effects, Sci. Rep-Uk., 8, 535, https://doi.org/10.1038/s41598-017-
- 963 18983-7, 2018.
- Li, J. J., Wang, G. H., Zhang, Q., Li, J., Wu, C., Jiang, W. Q., Zhu, T., and Zeng, L. M.: Molecular
- 965 characteristics and diurnal variations of organic aerosols at a rural site in the North China Plain with
- 966 implications for the influence of regional biomass burning, Atmos. Chem. Phys., 19, 10481-
- 967 https://doi.org/10496, 10.5194/acp-19-10481-2019, 2019.
- Lin, Y. H., Zhang, Z., Docherty, K. S., Zhang, H., Budisulistiorini, S. H., Rubitschun, C. L., Shaw, S. L.,
- Knipping, E. M., Edgerton, E. S., Kleindienst, T. E., Gold, A., and Surratt, J. D.: Isoprene Epoxydiols as
- 970 Precursors to Secondary Organic Aerosol Formation: Acid-Catalyzed Reactive Uptake Studies with
- 971 Authentic Compounds, Environ. Sci. Technol., 46, 250–258, https://doi.org/10.1021/es202554c, 2012.
- 272 Lin, Y. H., Knipping, E. M., Edgerton, E. S., Shaw, S. L., and Surratt, J. D.: Investigating the influences of
- SO<sub>2</sub> and NH<sub>3</sub> levels on isoprene-derived secondary organic aerosol formation using conditional sampling
- 974 approaches, Atmos. Chem. Phys., 13, 8457–8470, https://doi.org/10.5194/acp-13-8457-2013, 2013.

- 975 Liu, D., Xu, S. F., Lang, Y. C., Hou, S. J., Wei, L. F., Pan, X. L., Sun, Y. L., Wang, Z. F., Kawamura, K., and
- 976 Fu, P. Q.: Size distributions of molecular markers for biogenic secondary organic aerosol in urban Beijing,
- 977 Environ. Pollut., 327, 121569, https://doi.org/10.1016/j.envpol.2023.121569, 2023.
- Ng, N. L., Brown, S. S., Archibald, A. T., Atlas, E., Cohen, R. C., Crowley, J. N., Day, D. A., Donahue, N. M.,
- 979 Fry, J. L., Fuchs, H., Griffin, R. J., Guzman, M. I., Herrmann, H., Hodzic, A., Iinuma, Y., Jimenez, J. L.,
- Kiendler-Scharr, A., Lee, B. H., Luecken, D. J., Mao, J., McLaren, R., Mutzel, A., Osthoff, H. D., Ouyang,
- 981 B., Picquet-Varrault, B., Platt, U., Pye, H. O. T., Rudich, Y., Schwantes, R. H., Shiraiwa, M., Stutz, J.,
- 982 Thornton, J. A., Tilgner, A., Williams, B. J., and Zaveri, R. A.: Nitrate radicals and biogenic volatile
- organic compounds: oxidation, mechanisms, and organic aerosol, Atmos. Chem. Phys., 17, 2103–2162,
- 984 https://doi.org/10.5194/acp-17-2103-2017, 2017.
- 985 Nguyen, T. B., Bates, K. H., Crounse, J. D., Schwantes, R. H., Zhang, X., Kjaergaard, H. G., Surratt, J. D., Lin,
- P., Laskin, A., Seinfeld, J. H., and Wennberg, P. O.: Mechanism of the hydroxyl radical oxidation of
- 987 methacryloyl peroxynitrate (MPAN) and its pathway toward secondary organic aerosol formation in the
- 988 atmosphere, Chem. Phys., 17, 17914–17926, https://doi.org/10.1039/c5cp02001h, 2015.
- Nolte, C. G., Schauer, J. J., Cass, G. R., and Simoneit, B. R. T.: Highly Polar Organic Compounds Present in
- 990 Meat Smoke, Environ. Sci. Technol., 33, 3313–3316, https://doi.org/10.1021/es990122v, 1999.
- 991 Nolte, C. G., Schauer, J. J., Cass, G. R., and Simoneit, B. R. T.: Highly Polar Organic Compounds Present in
- 992 Wood Smoke and in the Ambient Atmosphere, Environ. Sci. Technol., 35, 1912–1919,
- 993 https://doi.org/10.1021/es001420r, 2001.
- 994 Nozi ère, B., Gonz ález, N. J. D., Borg-Karlson, A. K., Pei, Y. X., Redeby, J. P., Krejci, R., Dommen, J., Pr év ât,
- A. S. H., and Anthonsen, T.: Atmospheric chemistry in stereo: A new look at secondary organic aerosols
- 996 from isoprene, Geophys. Res. Lett., 38, https://doi.org/10.1029/2011GL047323, 2011.
- 997 Oros, D. R., and Simoneit, B. R. T.: Identification and emission rates of molecular tracers in coal smoke
- 998 particulate matter, Fuel, 79, 515–536, https://doi.org/10.1016/S0016-2361(99)00153-2, 2000.
- 999 Oros, D. R., and Simoneit, B. R. T.: Identification and emission factors of molecular tracers in organic aerosols
- from biomass burning Part 2. Deciduous trees, Appl. Geochem., 16, 1545–1565,
- 1001 https://doi.org/10.1016/S0883-2927(01)00022-1, 2001.
- 1002 Piccot, S. D., Watson, J. J., and Jones, J. W.: A global inventory of volatile organic compound emissions from
- anthropogenic sources, J. Geophys. Res., 97, 9897–9912, https://doi.org/10.1029/92JD00682, 1992.
- Puxbaum, H., and Tenze-Kunit, M.: Size distribution and seasonal variation of atmospheric cellulose, Atmos.
- 1005 Environ., 37, 3693–3699, https://doi.org/10.1016/S1352-2310(03)00451-5, 2003.

- 1006 Ren, H., Hu, W., Wei, L. F., Yue, S. Y., Zhao, J., Li, L. J., Wu, L. B., Zhao, W. Y., Ren, L. J., Kang, M. J., Xie,
- Q. Y., Su, S. H., Pan, X. L., Wang, Z. F., Sun, Y. L., Kawamura, K., and Fu, P. Q.: Measurement report:
- 1008 Vertical distribution of biogenic and anthropogenic secondary organic aerosols in the urban boundary layer
- over Beijing during late summer, Atmos. Chem. Phys., 21, 12949–12963, https://doi.org/10.5194/acp-21-
- 1010 12949-2021, 2021.
- 1011 Ren, Y. Q., Wang, G. H., Tao, J., Zhang, Z. S., Wu, C., Wang, J. Y., Li, J. J, Wei, J., Li, H., and Meng, F.:
- Seasonal characteristics of biogenic secondary organic aerosols at Mt. Wuyi in Southeastern China:
- 1013 Influence of anthropogenic pollutants, Environ. Pollut., 252, 493–500,
- 1014 https://doi.org/10.1016/j.envpol.2019.05.077, 2019.
- Riipinen, I., Yli-Juuti, T., Pierce, J. R., Petaja, T., Worsnop, D. R., Kulmala, M., and Donahue, N. M.: The
- 1016 contribution of organics to atmospheric nanoparticle growth, Nat. Geosci., 5, 453–458,
- 1017 https://doi.org/10.1038/ngeo1499, 2012.
- Rogge, W. F., Hildemann, L. M., Mazurek, M. A., Cass, G. R., and Simoneit, B. R. T.: Sources of fine organic
- aerosol. 1. Charbroilers and meat cooking operations, Environ. Sci. Technol., 25, 1112-1125,
- 1020 https://doi.org/10.1021/es00018a015, 1991.
- Rogge, W. F., Hildemann, L. M., Mazurek, M. A., Cass, G. R., Simoneit, B. R. T. J. E. S., and Technology:
- Sources of fine organic aerosol. 2. Noncatalyst and catalyst-equipped automobiles and heavy-duty diesel
- 1023 trucks, Environ. Sci. Technol., 27, 636–651, https://doi.org/10.1021/es00041a007, 1993a.
- Rogge, W. F., Hildemann, L. M., Mazurek, M. A., Cass, G. R., and Simoneit, B. R. T.: Sources of fine organic
- aerosol. 4. Particulate abrasion products from leaf surfaces of urban plants, Environ. Sci. Technol., 27,
- 1026 2700–2711, https://doi.org/10.1021/es00049a008, 1993b.
- 1027 Rogge, W. F., Medeiros, P. M., and Simoneit, B. R. T.: Organic marker compounds for surface soil and
- fugitive dust from open lot dairies and cattle feedlots, Atmos. Environ., 40, 27-49,
- 1029 https://doi.org/10.1016/j.atmosenv.2005.07.076, 2006.
- Rudich, Y., Donahue, N. M., and Mentel, T. F.: Aging of organic aerosol: bridging the gap between laboratory
- 1031 and field studies, Annu. Rev. Phys. Chem., 58, 321–352,
- https://doi.org/10.1146/annurev.physchem.58.032806.104432, 2007.
- 1033 Rybicki, M., Marynowski, L., Bechtel, A., and Simoneit, B. R. T.: Variations in δ13C values of levoglucosan
- from low-temperature burning of lignite and biomass, Sci. Total Environ., 733, 138991,
- 1035 https://doi.org/10.1016/j.scitotenv.2020.138991, 2020a.

- 1036 Rybicki, M., Marynowski, L., and Simoneit, B. R. T.: Composition of organic compounds from low-
- temperature burning of lignite and their application as tracers in ambient air, Chemosphere, 249, 126087,
- 1038 https://doi.org/10.1016/j.chemosphere.2020.126087, 2020b.
- Saarikoski, S., Timonen, H., Saarnio, K., Aurela, M., Järvi, L., Keronen, P., Kerminen, V. M., and Hillamo, R.:
- Sources of organic carbon in fine particulate matter in northern European urban air, Atmos. Chem. Phys., 8,
- 1041 6281–6295, https://doi.org/10.5194/acp-8-6281-2008, 2008.
- 1042 Sharkey, T. D., Wiberley, A. E., and Donohue, A. R.: Isoprene emission from plants: why and how, Annals of
- 1043 botany, 101, 5–18, https://doi.org/10.1093/aob/mcm240, 2008.
- Sheesley, R. J., Schauer, J. J., Chowdhury, Z., Cass, G. R., and Simoneit, B. R. T.: Characterization of organic
- aerosols emitted from the combustion of biomass indigenous to South Asia, J. Geophys. Res-Atmos., 108,
- 1046 https://doi.org/10.1029/2002JD002981, 2003.
- 1047 Shiraiwa, M., Ueda, K., Pozzer, A., Lammel, G., Kampf, C. J., Fushimi, A., Enami, S., Arangio, A. M.,
- Fröhlich-Nowoisky, J., Fujitani, Y., Furuyama, A., Lakey, P. S. J., Lelieveld, J., Lucas, K., Morino, Y.,
- Pöschl, U., Takahama, S., Takami, A., Tong, H., Weber, B., Yoshino, A., and Sato, K.: Aerosol Health
- 1050 Effects from Molecular to Global Scales, Environ. Sci. Technol., 51, 13545–13567,
- 1051 10.1021/acs.est.7b04417, 2017.
- 1052 Simoneit, B. R. T.: Biomass burning a review of organic tracers for smoke from incomplete combustion,
- 1053 Applied Geochemistry, 17, 129–162, https://doi.org/10.1016/S0883-2927(01)00061-0, 2002.
- Simoneit, B. R. T., Kobayashi, M., Mochida, M., Kawamura, K., and Huebert, B. J.: Aerosol particles
- 1055 collected on aircraft flights over the northwestern Pacific region during the ACE-Asia campaign:
- 1056 Composition and major sources of the organic compounds, J. Geophys. Res-Atmos., 109,
- 1057 https://doi.org/10.1029/2004JD004565, 2004a.
- Simoneit, B. R., Elias, V. O., Kobayashi, M., Kawamura, K., Rushdi, A. I., Medeiros, P. M., Rogge, W. F.,
- and Didyk, B. M.: Sugars-dominant water-soluble organic compounds in soils and characterization as
- tracers in atmospheric particulate matter, Environ. Sci. Technol., 38, 5939–5949,
- 1061 https://doi.org/10.1021/es0403099, 2004b.
- 1062 Srivastava, D., Vu, T. V., Tong, S., Shi, Z., and Harrison, R. M.: Formation of secondary organic aerosols
- from anthropogenic precursors in laboratory studies, Npj. Clim. Atmos. Sci., 5, 22,
- 1064 https://doi.org/10.1038/s41612-022-00238-6, 2022.
- Stohl, A., Berg, T., Burkhart, J. F., Fjáraa, A. M., Forster, C., Herber, A., Hov, Ø., Lunder, C., McMillan, W.
- W., Oltmans, S., Shiobara, M., Simpson, D., Solberg, S., Stebel, K., Ström, J., Tørseth, K., Treffeisen, R.,
- 1067 Virkkunen, K., and Yttri, K. E.: Arctic smoke record high air pollution levels in the European

- Arctic due to agricultural fires in Eastern Europe in spring 2006, Atmos. Chem. Phys., 7, 511-534,
- 1069 https://doi.org/10.5194/acp-7-511-2007, 2007.
- 1070 Stone, E. A., Zhou, J., Snyder, D. C., Rutter, A. P., Mieritz, M., and Schauer, J. J.: A comparison of
- summertime secondary organic aerosol source contributions at contrasting urban locations, Environ. Sci.
- Technol., 43, 3448–3454, https://doi.org/10.1021/es8025209, 2009.
- 1073 Surratt, J. D., Murphy, S. M., Kroll, J. H., Ng, N. L., Hildebrandt, L., Sorooshian, A., Szmigielski, R.,
- Vermeylen, R., Maenhaut, W., Claeys, M., Flagan, R. C., and Seinfeld, J. H.: Chemical Composition of
- Secondary Organic Aerosol Formed from the Photooxidation of Isoprene, J. Phys. Chem. A, 110, 9665–
- 1076 9690, 10.1021/jp061734m, 2006.
- 1077 Surratt, J. D., Chan, A. W. H., Eddingsaas, N. C., Chan, M., Loza, C. L., Kwan, A. J., Hersey, S. P., Flagan, R.
- 1078 C., Wennberg, P. O., and Seinfeld, J. H.: Reactive intermediates revealed in secondary organic aerosol
- formation from isoprene, Proc. Natl. Acad. Sci. U.S.A., 107, 6640-6645,
- 1080 https://doi.org/doi:10.1073/pnas.0911114107, 2010.
- Tang, T. G., Cheng, Z. N., Xu, B. Q., Zhang, B. L., Li, J., Zhang, W., Wang, K. L., and Zhang, G.: Source
- Diversity of Intermediate Volatility n-Alkanes Revealed by Compound-Specific δ<sup>13</sup>C-δD Isotopes, Environ.
- 1083 Sci. Technol., 56, 14262–14271, 10.1021/acs.est.2c02156, 2022.
- 1084 Tong, D., Cheng, J., Liu, Y., Yu, S., Yan, L., Hong, C., Qin, Y., Zhao, H., Zheng, Y., Geng, G., Li, M., Liu, F.,
- Zhang, Y., Zheng, B., Clarke, L., and Zhang, Q.: Dynamic projection of anthropogenic emissions in China:
- methodology and 2015–2050 emission pathways under a range of socio-economic, climate policy, and
- pollution control scenarios, Atmos. Chem. Phys., 20, 5729–5757, https://doi.org/10.5194/acp-20-5729-
- 1088 2020, 2020.
- Turpin, B. J., and Huntzicker, J. J.: Identification of secondary organic aerosol episodes and quantitation of
- primary and secondary organic aerosol concentrations during SCAQS, Atmos. Environ., 29, 3527–3544,
- 1091 https://doi.org/10.1016/1352-2310(94)00276-Q, 1995.
- von Schneidemesser, E., Zhou, J., Stone, E. A., Schauer, J. J., Shpund, J., Brenner, S., Qasrawi, R., Abdeen, Z.,
- and Sarnat, J. A.: Spatial Variability of Carbonaceous Aerosol Concentrations in East and West Jerusalem,
- Environ. Sci. Technol., 44, 1911–1917, https://doi.org/10.1021/es9014025, 2010.
- 1095 Wang, G. H., and Kawamura, K.: Molecular Characteristics of Urban Organic Aerosols from Nanjing: A Case
- 1096 Study of A Mega-City in China, Environ. Sci. Technol., 39, 7430–7438, https://doi.org/10.1021/es051055,
- 1097 2005.

- Wang, G. H., Kawamura, K., Lee, S., Ho, K., and Cao, J. J.: Molecular, Seasonal, and Spatial Distributions of
- Organic Aerosols from Fourteen Chinese Cities, Environ. Sci. Technol., 40, 4619-4625,
- 1100 https://doi.org/10.1021/es060291x, 2006.
- Wang, G. H., Kawamura, K., Hatakeyama, S., Takami, A., Li, H., and Wang, W.: Aircraft Measurement of
- Organic Aerosols over China, Environ. Sci. Technol., 41, 3115–3120, https://doi.org/10.1021/es062601h,
- 1103 2007.
- Wang, Q., Shao, M., Zhang, Y., Wei, Y., Hu, M., and Guo, S.: Source apportionment of fine organic aerosols
- in Beijing, Atmos. Chem. Phys., 9, 8573–8585, https://doi.org/10.5194/acp-9-8573-2009, 2009.
- 1106 Wang, Y., Pavuluri, C. M., Fu, P. Q., Li, P. S., Dong, Z. C., Xu, Z. J., Ren, H., Fan, Y. B., Li, L. J., Zhang, Y.
- 1107 L., and Liu, C. Q.: Characterization of Secondary Organic Aerosol Tracers over Tianjin, North China
- during Summer to Autumn, Acs Earth Space Chem., 3, 2339–2352, 10.1021/acsearthspacechem.9b00170,
- 1109 2019.
- 1110 Wang, Z., Wu, D., Li, Z., Shang, X., Li, Q., Li, X., Chen, R., Kan, H., Ouyang, H., Tang, X., and Chen, J.:
- 1111 Measurement report: Saccharide composition in atmospheric fine particulate matter during spring at the
- remote sites of southwest China and estimates of source contributions, Atmos, Chem. Phys., 21, 12227–
- 1113 12241, https://doi.org/10.5194/acp-21-12227-2021, 2021.
- Weber, R. J., Sullivan, A. P., Peltier, R. E., Russell, A. G., Yan, B., Zheng, M., Gouw, J. d., Warneke, C.,
- Brock, C. A., Holloway, J. S., Atlas, E. L., and Edgerton, E. S.: A study of secondary organic aerosol
- formation in the anthropogenic-influenced southeastern United States, J. Geophys. Res-Atmos., 112,
- 1117 https://doi.org/10.1029/2007JD008408, 2007.
- 1118 Wu, J. R., Bei, N. F., Wang, Y., Li, X., Liu, S. X., Liu, L., Wang, R. N., Yu, J. Y., Le, T. H., Zuo, M., Shen, Z.
- 1119 X., Cao, J. J., Tie, X. X., and Li, G. H.: Insights into particulate matter pollution in the North China Plain
- during wintertime: local contribution or regional transport?, Atmos. Chem. Phys., 21, 2229-2249,
- https://doi.org/10.5194/acp-21-2229-2021, 2021.
- 1122 Wu, X., Chen, C., Vu, T. V., Liu, D., Baldo, C., Shen, X., Zhang, Q., Cen, K., Zheng, M., He, K., Shi, Z., and
- Harrison, R. M.: Source apportionment of fine organic carbon (OC) using receptor modelling at a rural site
- of Beijing: Insight into seasonal and diurnal variation of source contributions, Environ. Pollut., 266, 115078,
- https://doi.org/10.1016/j.envpol.2020.115078, 2020.
- 1126 Xu, B. Q., Tang, J., Tang, T. G., Zhao, S. Z., Zhong, G. C., Zhu, S. Y., Li, J., and Zhang, G.: Fates of
- secondary organic aerosols in the atmosphere identified from compound-specific dual-carbon isotope
- analysis of oxalic acid, Atmos. Chem. Phys., 23, 1565–1578, https://doi.org/10.5194/acp-23-1565-2023,
- 1129 2023.

- Xu, B. Q., Zhang, G., Gustafsson, Ö., Kawamura, K., Li, J., Andersson, A., Bikkina, S., Kunwar, B., Pokhrel,
- 1131 A., Zhong, G. C., Zhao, S. Z., Li, J., Huang, C., Cheng, Z. N., Zhu, S. Y., Peng, P. A., and Sheng, G. Y.:
- Large contribution of fossil-derived components to aqueous secondary organic aerosols in China, Nat.
- 1133 Commun., 13, 5115, https://doi.org/10.1038/s41467-022-32863-3, 2022.
- 1134 Xu, J. S., Liu, D., Wu, X. F., Vu, T. V., Zhang, Y. L., Fu, P. Q., Sun, Y. L., Xu, W. Q., Zheng, B., Harrison, R.
- 1135 M., and Shi, Z. B.: Source apportionment of fine organic carbon at an urban site of Beijing using a
- 1136 chemical mass balance model, Atmos. Chem. Phys., 21, 7321–7341, https://doi.org/10.5194/acp-21-7321-
- 1137 2021, 2021.
- 1138 Xu, S. F., Ren, L. J., Lang, Y. C., Hou, S. J., Ren, H., Wei, L. F., Wu, L. B., Deng, J. J., Hu, W., Pan, X. L.,
- Sun, Y., Wang, Z. F., Su, H., Cheng, Y. F., and Fu, P. Q: Molecular markers of biomass burning and
- primary biological aerosols in urban Beijing: size distribution and seasonal variation, Atmos. Chem. Phys.,
- 20, 3623–3644, https://doi.org/10.5194/acp-20-3623-2020, 2020.
- Yan, C. C., Sullivan, A. P., Cheng, Y., Zheng, M., Zhang, Y. H., Zhu, T., and Collett, J. L.: Characterization of
- saccharides and associated usage in determining biogenic and biomass burning aerosols in atmospheric fine
- particulate matter in the North China Plain, Sci. Total Environ., 650, 2939–2950,
- https://doi.org/10.1016/j.scitotenv.2018.09.325, 2019.
- Yang, C., Hong, Z. Y., Chen, J. S., Xu, L. L., Zhuang, M. Z., and Huang, Z.: Characteristics of secondary
- organic aerosols tracers in PM2.5 in three central cities of the Yangtze river delta, China, Chemosphere,
- 293, 133637, https://doi.org/10.1016/j.chemosphere.2022.133637, 2022.
- 1149 Yazdani, A., Dudani, N., Takahama, S., Bertrand, A., Prévât, A. S. H., El Haddad, I., and Dillner, A. M.:
- 1150 Characterization of primary and aged wood burning and coal combustion organic aerosols in an
- environmental chamber and its implications for atmospheric aerosols, Atmos. Chem. Phys., 21, 10273–
- 1152 10293, https://doi.org/10.5194/acp-21-10273-2021, 2021.
- Yee, L. D., Isaacman-VanWertz, G., Wernis, R. A., Kreisberg, N. M., Glasius, M., Riva, M., Surratt, J. D., de
- Sá, S. S., Martin, S. T., Alexander, M. L., Palm, B. B., Hu, W., Campuzano-Jost, P., Day, D. A., Jimenez, J.
- L., Liu, Y., Misztal, P. K., Artaxo, P., Viegas, J., Manzi, A., de Souza, R. A. F., Edgerton, E. S., Baumann,
- 1156 K., and Goldstein, A. H.: Natural and Anthropogenically Influenced Isoprene Oxidation in Southeastern
- 1157 United States and Central Amazon, Environ. Sci. Technol., 54, 5980-5991,
- 1158 https://doi.org/10.1021/acs.est.0c00805, 2020.
- 1159 Yttri, K. E., Dye, C., and Kiss, G.: Ambient aerosol concentrations of sugars and sugar-alcohols at four
- different sites in Norway, Atmos. Chem. Phys., 7, 4267–4279, https://doi.org/10.5194/acp-7-4267-2007,
- 1161 2007.

- 1162 Yuan, Q., Lai, S. C., Song, J. W., Ding, X., Zheng, L. S., Wang, X. M., Zhao, Y., Zheng, J. Y., Yue, D. L.,
- Zhong, L. J., Niu, X. J., and Zhang, Y. Y.: Seasonal cycles of secondary organic aerosol tracers in rural
- Guangzhou, Southern China: The importance of atmospheric oxidants, Environ. Pollut., 240, 884–893,
- https://doi.org/10.1016/j.envpol.2018.05.009, 2018.
- 1166 Zhang, Q., He, K. B., and Huo, H.: Cleaning China's air, Nature, 484, 161-162,
- 1167 https://doi.org/10.1038/484161a, 2012.
- 1168 Zhang, Q., Hu, W., Ren, H., Yang, J. B., Deng, J. J., Wang, D. W., Sun, Y. L., Wang, Z. F., Kawamura, K.,
- and Fu, P. Q.: Diurnal variations in primary and secondary organic aerosols in an eastern China coastal city:
- 1170 The impact of land-sea breezes, Environ. Pollut., 319, 121016,
- https://doi.org/10.1016/j.envpol.2023.121016, 2023.
- Zhang, S., Gong, D., Wu, G., Li, Y., Ding, Y., Wang, B., and Wang, H.: Molecular characteristics and
- formation mechanisms of biogenic secondary organic aerosols in the mountainous background atmosphere
- of southern China, Atmos. Environ., 329, 120540, https://doi.org/10.1016/j.atmosenv.2024.120540, 2024.
- Zhang, X., McVay, R. C., Huang, D. D., Dalleska, N. F., Aumont, B., Flagan, R. C., and Seinfeld, J. H.:
- Formation and evolution of molecular products in α-pinene secondary organic aerosol, Proc. Natl. Acad.
- 1177 Sci. U. S. A., 112, 14168–14173, https://doi.org/10.1073/pnas.1517742112, 2015.
- 1178 Zhang, Y. X., Cao, F., Song, W. H., Jia, X. F., Xie, T., Wu, C.L., Yan, P., Yu, M. Y., Rauber, M., Salazar, G.,
- 1179 Szidat, S., and Zhang, Y. L.: Fossil and Nonfossil Sources of Winter Organic Aerosols in the Regional
- Background Atmosphere of China, Environ. Sci. Technol., 58, 1244–1254,
- 1181 https://doi.org/10.1021/acs.est.3c08491, 2024.
- Zhang, Y. X., Schauer, J. J., Zhang, Y. H., Zeng, L. M., Wei, Y. J., Liu, Y., and Shao, M.: Characteristics of
- Particulate Carbon Emissions from Real-World Chinese Coal Combustion, Environ. Sci. Technol., 42,
- 5068–5073, https://doi.org/10.1021/es7022576, 2008.
- 2 Zhang, Y. L., Kawamura, K., Agrios, K., Lee, M., Salazar, G., and Szidat, S.: Fossil and Nonfossil Sources of
- Organic and Elemental Carbon Aerosols in the Outflow from Northeast China, Environ. Sci. Technol., 50,
- 1187 6284–6292, https://doi.org/10.1021/acs.est.6b00351, 2016.
- 2 Zhang, Y. X., Shao, M., Zhang, Y.H., Zeng, L.M., He, L.Y., Zhu, B., Wei, Y.J., and Zhu, X.L.: Source profiles
- of particulate organic matters emitted from cereal straw burnings, J. Environ. Sci., 19, 167–175,
- https://doi.org/10.1016/S1001-0742(07)60027-8, 2007.
- 21191 Zheng, M., Cass, G. R., Schauer, J. J., and Edgerton, E. S.: Source apportionment of PM2.5 in the
- Southeastern United States using solvent-extractable organic compounds as tracers, Environ. Sci. Technol.,
- 36, 2361–2371, https://doi.org/10.1021/es011275x, 2002.

- Zhao, X., Hu, Q., Wang, X., Ding, X., He, Q., Zhang, Z., Shen, R., Lü, S., Liu, T., Fu, X., and Chen, L.:
- 1195 Composition profiles of organic aerosols from Chinese residential cooking: case study in urban Guangzhou,
- 1196 south China, J. Atmos. Chem., 72, 1–18, https://doi.org/10.1007/s10874-015-9298-0, 2015.
- Zhao, Y. L., Hu, M., Slanina, S., and Zhang, Y. H.: Chemical Compositions of Fine Particulate Organic Matter
- Emitted from Chinese Cooking, Environ. Sci. Technol., 41, 99–105, https://doi.org/10.1021/es0614518,
- 1199 2007.
- 1200 Zhu, C. M., Kawamura, K., and Fu, P. Q.: Seasonal variations of biogenic secondary organic aerosol tracers in
- 1201 Cape Hedo, Okinawa, Atmos. Environ., 130, 113–119, https://doi.org/10.1016/j.atmosenv.2015.08.069,
- 1202 2016.
- 1203 Zhu, R. G., Xiao, H. Y., Cheng, L., Zhu, H., Xiao, H., and Gong, Y. Y.: Measurement report: Characterization
- of sugars and amino acids in atmospheric fine particulates and their relationship to local primary sources,
- 1205 Atmos. Chem. Phys., 22, 14019–14036, 10.5194/acp-22-14019-2022, 2022.

## Figure Captions

1226

1227 Figure 1. One-year time series of organic carbon (OC), elemental carbon (EC), OC/EC ratios, PM<sub>2.5</sub> levels, and 1228 concentrations of polar organic compounds. Figure 2. Molecular characteristics and seasonal variations of the major polar compounds in PM<sub>2.5</sub>. The bars in 1229 1230 the figure show the average concentrations of different compounds for each season, while the caps on the bars 1231 represent the standard deviations of these averages. The letters a, b, c, and d above the caps indicate whether 1232 the average concentrations differ significantly between seasons. Data points that do not share the same letter 1233 are significantly different, whereas those with the same letter are not significantly different, at the 95% 1234 confidence level. The Tukey test was used to assess the statistical significance of these differences. It should be 1235 noted that the same method was used to compare the statistical significance of differences between the data in 1236 the other figures presented later in the article. 1237 Figure 3. Molecular characteristics and seasonal variations of the minor polar compounds in PM<sub>2.5</sub>. The 1238 explanations for the letters a, b, c, and d on the bars are provided in the caption of Figure 2. Figure 4. Molecular characteristics and seasonal variations of the SOA tracers in PM<sub>2.5</sub>. The explanations for 1239 1240 the letters a, b, c, and d on the bars are provided in the caption of Figure 2. 1241 Figure 5. Concentrations and relative abundances of primary organic carbon (POC) from biomass burning 1242 (POC<sub>bb</sub>), coal combustion (POC<sub>cc</sub>), vehicle exhaust (POC<sub>ve</sub>), cooking (POC<sub>c</sub>), plant debris (POC<sub>pd</sub>), and fungal 1243 spores (POC<sub>fs</sub>), as well as secondary organic carbon (SOC) from isoprene (SOC<sub>i</sub>), α/β-pinene (SOC<sub>p</sub>), β-1244 caryophyllene (SOC<sub>t</sub>), toluene (SOC<sub>t</sub>), and naphthalene (SOC<sub>n</sub>). POC and SOC concentrations were estimated 1245 using a tracer-based method, while other organic carbon (OOC) was calculated by subtracting the estimated 1246 OC from the measured OC. Winter-P refers to winter pollution periods, and Winter-R denotes the winter 1247 remainder. 1248 Figure 6. Pearson correlations between POC, SOC, and the measured OC for the annual sampling period (a), 1249 winter pollution periods (b), winter remainder (c), and individual pollution episodes in winter (d-l). The size of 1250 each circle represents the contribution (%) of POC and SOC to the variation in measured OC, as determined by 1251 redundancy analysis. Magenta circles indicate P-values from correlation and redundancy analyses less than 0.05, while gray circles denote P-values greater than 0.05. Definitions: POC<sub>bb</sub> (biomass burning), POC<sub>cc</sub> (coal 1252

combustion), POCve (vehicle exhaust), POCc (cooking), POCpd (plant debris), POCfs (fungal spores), and POC<sub>EC-based</sub> (based on the EC method). SOC<sub>i</sub>, SOC<sub>p</sub>, SOC<sub>c</sub>, SOC<sub>t</sub>, SOC<sub>n</sub>, and SOC<sub>EC-based</sub> correspond to SOC from isoprene,  $\alpha/\beta$ -pinene,  $\beta$ -caryophyllene, toluene, naphthalene, and EC-based methods, respectively. Figure 7. Linear correlations between temperature, NO<sub>2</sub>, and SOC for the annual sampling periods (a), winter pollution periods (b), winter remainder (c), and individual winter pollution episodes (d-l). SOC concentrations were estimated using a tracer-based method. Winter-P refers to the winter pollution periods, while Winter-R denotes the winter remainder. PE1-PE9 correspond to winter pollution episodes 1-9. Before conducting linear correlation analyses, the Shapiro-Wilk test was used to assess the normality of the data, and linear correlations were conducted only for datasets significantly conforming to a normal distribution (p > 0.05). 

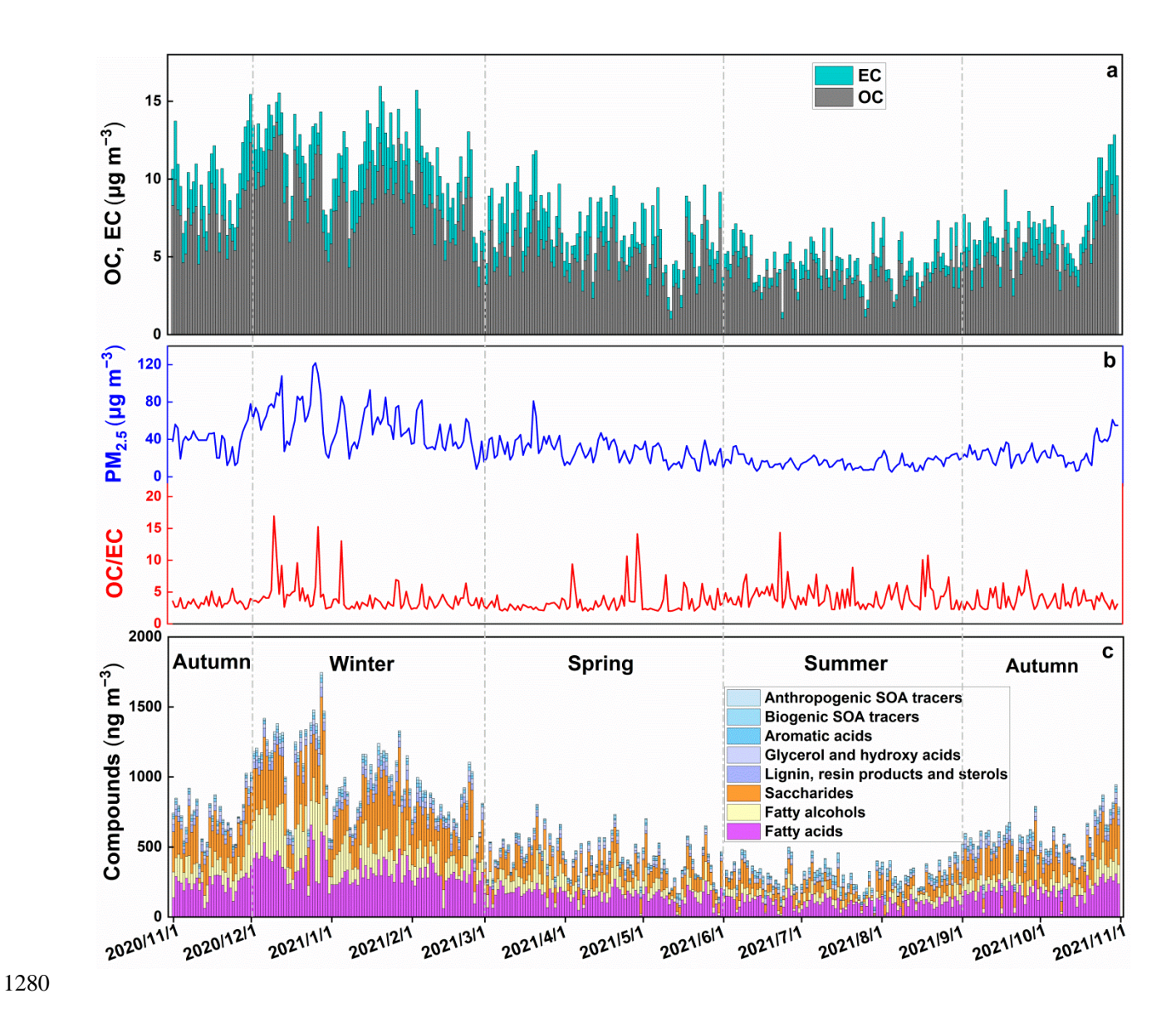


Figure 1. One-year time series of organic carbon (OC), elemental carbon (EC), OC/EC ratios, PM<sub>2.5</sub> levels, and concentrations of polar organic compounds.

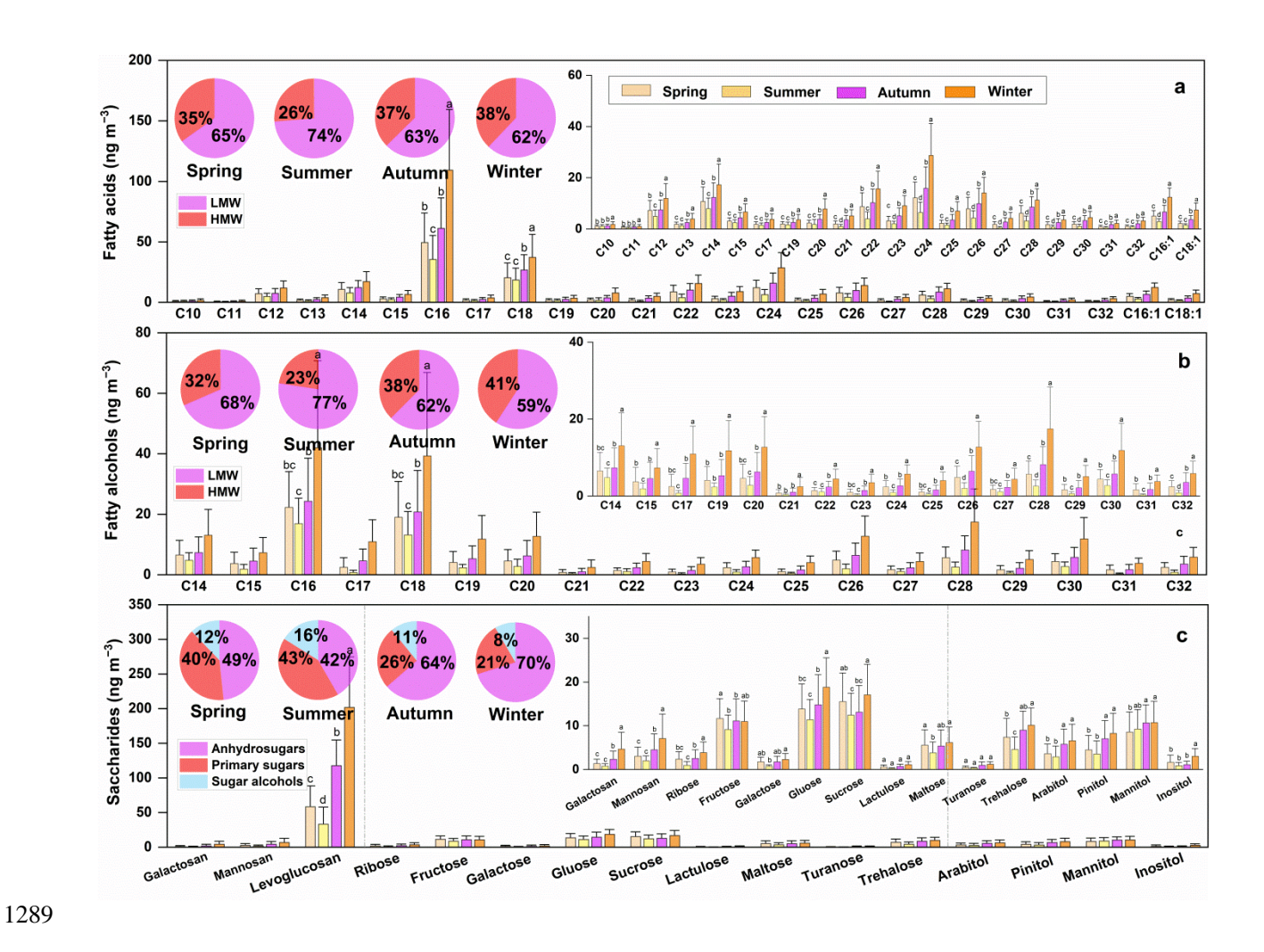


Figure 2. Molecular characteristics and seasonal variations of the major polar compounds in PM<sub>2.5</sub>. The bars in the figure show the average concentrations of different compounds for each season, while the caps on the bars represent the standard deviations of these averages. The letters a, b, c, and d above the caps indicate whether the average concentrations differ significantly between seasons. Data points that do not share the same letter are significantly different, whereas those with the same letter are not significantly different, at the 95% confidence level. The Tukey test was used to assess the statistical significance of these differences. It should be noted that the same method was used to compare the statistical significance of differences between the data in the other figures presented later in the article.

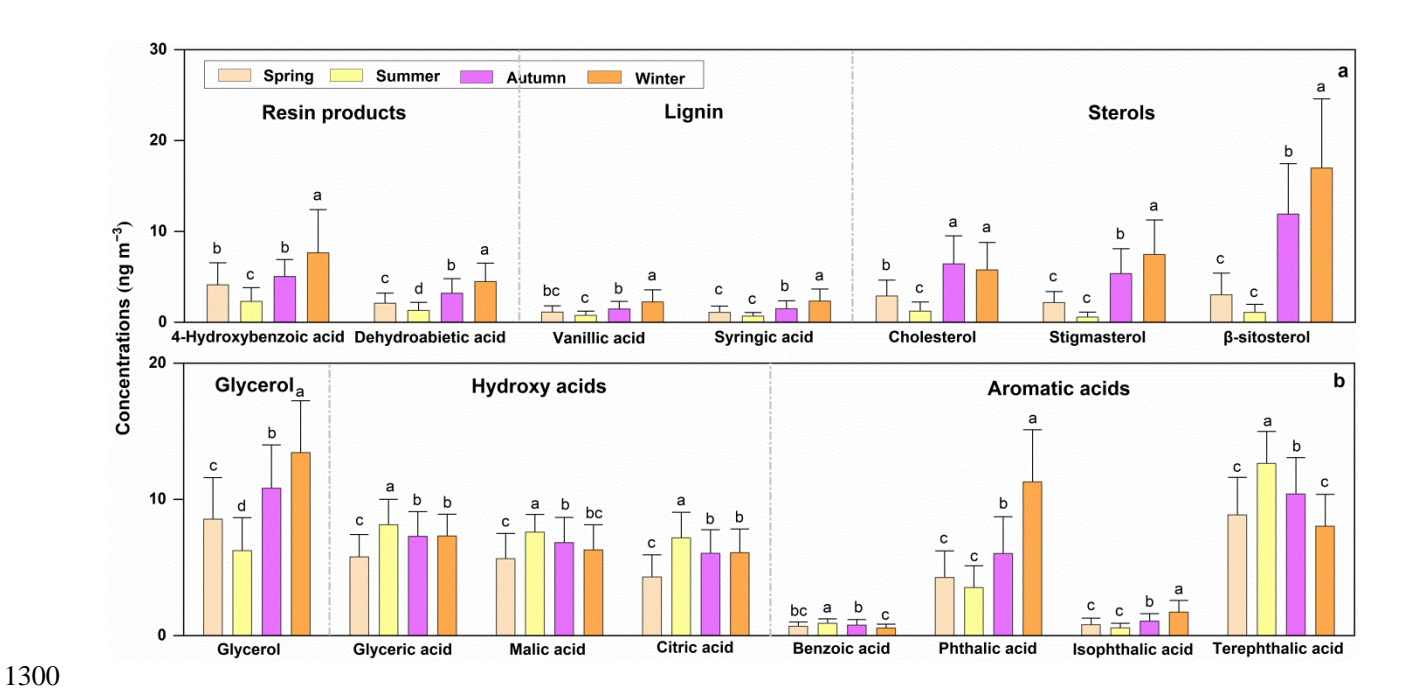


Figure 3. Molecular characteristics and seasonal variations of the minor polar compounds in  $PM_{2.5}$ . The explanations for the letters a, b, c, and d on the bars are provided in the caption of Figure 2.

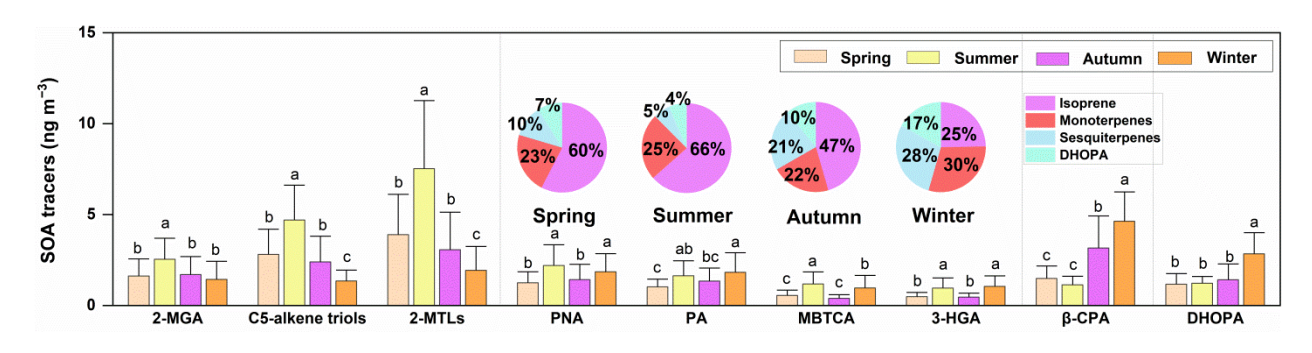


Figure 4. Molecular characteristics and seasonal variations of the SOA tracers in  $PM_{2.5}$ . The explanations for the letters a, b, c, and d on the bars are provided in the caption of Figure 2.

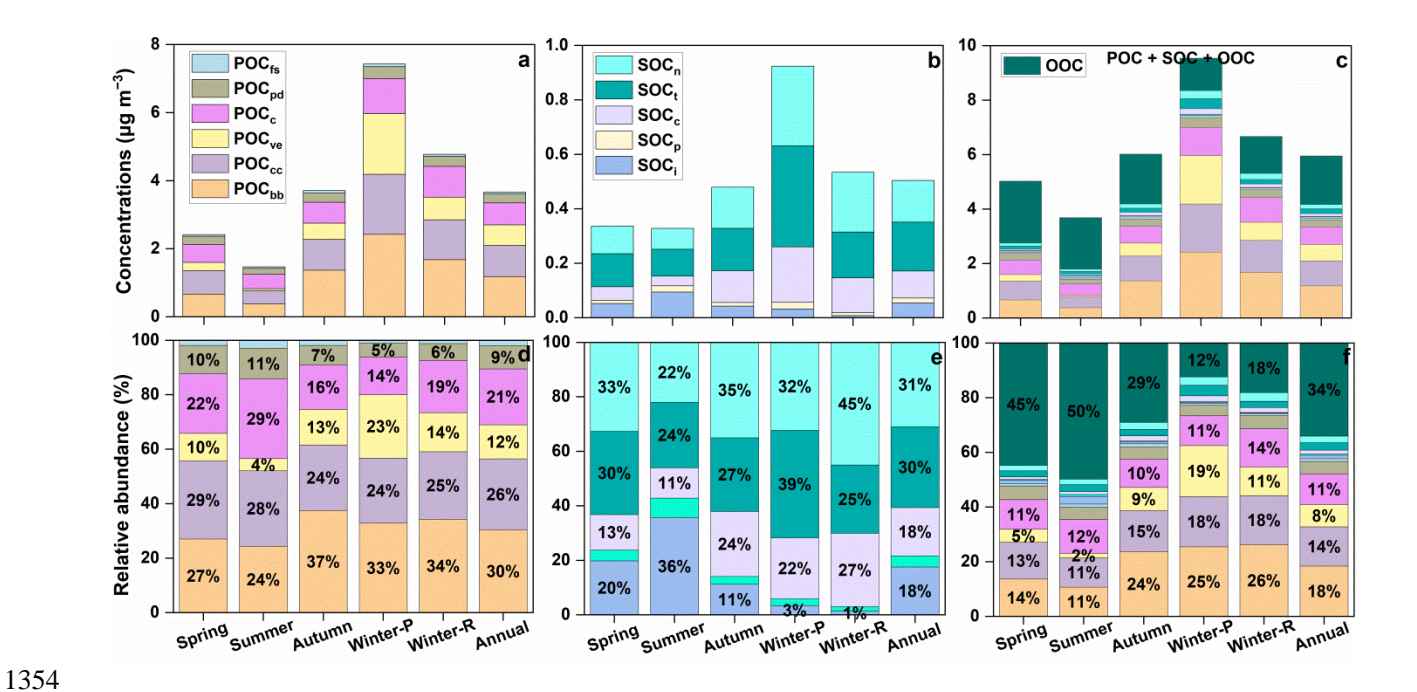


Figure 5. Concentrations and relative abundances of primary organic carbon (POC) from biomass burning (POC<sub>bb</sub>), coal combustion (POC<sub>cc</sub>), vehicle exhaust (POC<sub>ve</sub>), cooking (POC<sub>c</sub>), plant debris (POC<sub>pd</sub>), and fungal spores (POC<sub>fs</sub>), as well as secondary organic carbon (SOC) from isoprene (SOC<sub>i</sub>),  $\alpha/\beta$ -pinene (SOC<sub>p</sub>),  $\beta$ -caryophyllene (SOC<sub>c</sub>), toluene (SOC<sub>t</sub>), and naphthalene (SOC<sub>n</sub>). POC and SOC concentrations were estimated using a tracer-based method, while other organic carbon (OOC) was calculated by subtracting the estimated OC from the measured OC. Winter-P refers to winter pollution periods, and Winter-R denotes the winter remainder.

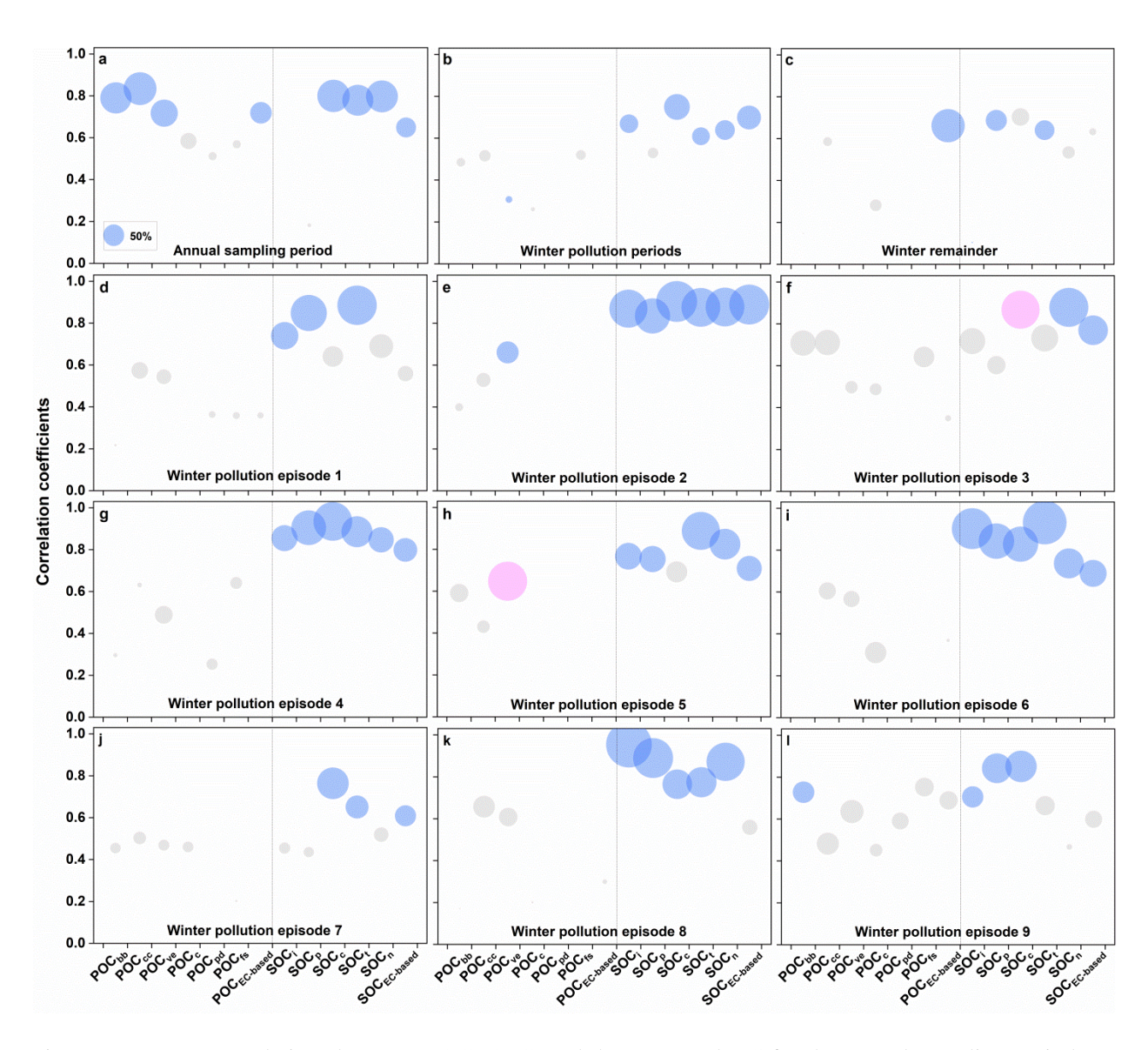


Figure 6. Pearson correlations between POC, SOC, and the measured OC for the annual sampling period (a), winter pollution periods (b), winter remainder (c), and individual pollution episodes in winter (d–l). The size of each circle represents the contribution (%) of POC and SOC to the variation in measured OC, as determined by redundancy analysis. Magenta circles indicate P-values from correlation and redundancy analyses less than 0.05, while gray circles denote P-values greater than 0.05. Definitions:  $POC_{bb}$  (biomass burning),  $POC_{cc}$  (coal combustion),  $POC_{ve}$  (vehicle exhaust),  $POC_{c}$  (cooking),  $POC_{pd}$  (plant debris),  $POC_{fs}$  (fungal spores), and  $POC_{EC-based}$  (based on the EC method).  $SOC_{i}$ ,  $SOC_{p}$ ,  $SOC_{c}$ ,  $SOC_{t}$ ,  $SOC_{n}$ , and  $SOC_{EC-based}$  correspond to SOC from isoprene,  $\alpha/\beta$ -pinene,  $\beta$ -caryophyllene, toluene, naphthalene, and EC-based methods, respectively.

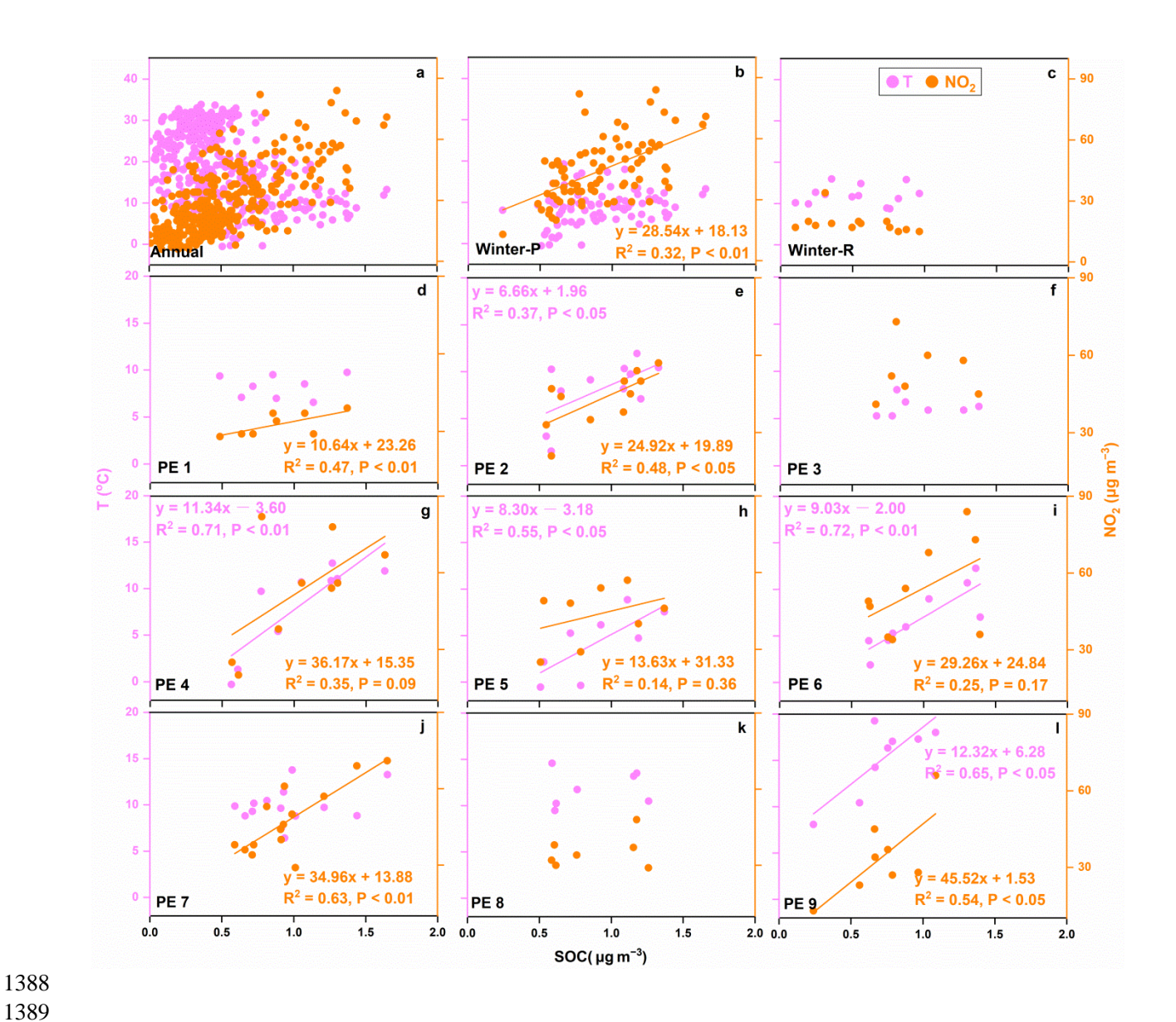


Figure 7. Linear correlations between temperature,  $NO_2$ , and SOC for the annual sampling periods (a), winter pollution periods (b), winter remainder (c), and individual winter pollution episodes (d–l). SOC concentrations were estimated using a tracer-based method. Winter-P refers to the winter pollution periods, while Winter-R denotes the winter remainder. PE1–PE9 correspond to winter pollution episodes 1–9. Before conducting linear correlation analyses, the Shapiro-Wilk test was used to assess the normality of the data, and linear correlations were conducted only for datasets significantly conforming to a normal distribution (p > 0.05).